

---

# COMPUTATIONALLY EFFICIENT APPROXIMATIONS FOR MATRIX-BASED RÉNYI'S ENTROPY

---

✉ **Tieliang Gong\***, **Yuxin Dong\***

School of Computer Science and Technology  
Xi'an Jiaotong University  
adidasglt@gmail.com, gamepiaynmo@gmail.com

**Shujian Yu**

Machine Learning Group  
UiT - The Arctic University of Norway  
yusj@9011@gmail.com

**Bo Dong**

School of Continuing Education  
Xi'an Jiaotong University  
dong.bo@mail.xjtu.edu.cn

## ABSTRACT

The recently developed matrix-based Rényi's  $\alpha$ -order entropy enables measurement of information in data simply using the eigenspectrum of symmetric positive semi-definite (PSD) matrices in reproducing kernel Hilbert space, without estimation of the underlying data distribution. This intriguing property makes this new information measurement widely adopted in multiple statistical inference and learning tasks. However, the computation of such quantity involves the trace operator on a PSD matrix  $\mathbf{G}$  to power  $\alpha$  (i.e.,  $\text{tr}(\mathbf{G}^\alpha)$ ), with a normal complexity of nearly  $O(n^3)$ , which severely hampers its practical usage when the number of samples (i.e.,  $n$ ) is large. In this work, we present computationally efficient approximations to this new entropy functional that can reduce its complexity to even significantly less than  $O(n^2)$ . To this end, we leverage the recent progress on Randomized Numerical Linear Algebra, developing Taylor, Chebyshev and Lanczos approximations to  $\text{tr}(\mathbf{G}^\alpha)$  for arbitrary values of  $\alpha$  by converting it into matrix-vector multiplications problem. We also establish the connection between the matrix-based Rényi's entropy and PSD matrix approximation, which enables exploiting both clustering and block low-rank structure of  $\mathbf{G}$  to further reduce the computational cost. We theoretically provide approximation accuracy guarantees and illustrate the properties of different approximations. Large-scale experimental evaluations on both synthetic and real-world data corroborate our theoretical findings, showing promising speedup with negligible loss in accuracy.

**Keywords** Matrix-based Rényi's Entropy, Randomized Numerical Linear Algebra, Trace Estimation, Information Bottleneck, Mutual Information.

## 1 Introduction

Over the past decades, the utilization of information theoretic measure has been extensively explored in information theory and machine learning communities, ranging from entropy Principe [2010], Li and Wu [2019] mutual information [Hjelm et al., 2018, Tschannen et al., 2019, Cheng and Carin., 2020] to information bottleneck TISHBY [1999], Alemi et al. [2016], Ngampruetikorn and Schwab [2021]. In most applications, exactly access to these measures usually involves estimation of the probability density function (PDF) of data, which is computation infeasible, especially in high dimensional space [Fan and Li, 2006].

In [Giraldo et al., 2014, Giraldo and Principe, 2014], a novel information measure, named matrix-based Rényi's  $\alpha$ -order entropy was proposed, which enables us quantify the information (or interactions) in variables directly from given samples. Distinct from the classic entropy information definitions (e.g. Shannon, Rényi entropy) which rely on

---

\*These authors contributed equally

probability densities, it is defined on the eigenspectrum of a Gram matrix constructed by projecting data in reproducing kernel Hilbert space (RKHS), thus avoiding the evaluation of underlying distribution. This attractive property leads to a variety of applications for matrix-based Rényi’s entropy [Brockmeier et al., 2017, Alvarez-Meza et al., 2017, Yu et al., 2019]. Moreover, it has also been recently used in advanced deep learning problems such as the analysis of learning dynamics of convolution neural networks [Wickstrøm et al., 2019] and the robust learning against covariant shift [Yu et al., 2021a].

Despite of its practical utility, estimating matrix-based Rényi’s entropy involves calculating eigenvalues of a Gram matrix  $G$  of size  $n \times n$  (where  $n$  is the sample size, please refer to Definition 1), which usually requires a computational complexity of  $O(n^3)$  with traditional techniques such as Singular Value Decomposition (SVD) [Elad, 2010, Li et al., 2014], CUR decomposition [Mahoney and Drineas, 2009, Mahoney, 2011] and QR Factorization [Watkins, 2008, 2004]. This drawback poses great challenges for both storage and computing in practice. We therefore seek for computationally efficient methods with statistical guarantees to approximate the matrix-based Rényi’s entropy. To this end, we borrow the idea of trace estimation Avron and Toledo [2011] to design a randomized approximation algorithm for matrix-based Rényi’s entropy with integer order  $\alpha$ , where we transfer matrix trace estimation into a matrix-vector multiplication problem. We further employ Taylor and Chebyshev series to approximate the power of  $G$  for fractional-order  $\alpha$ . Moreover, we establish the connection between matrix-based Rényi’s entropy and Gram matrix approximation, where we employ  $k$ -means to construct a block structure of  $G$  and use a low-rank decomposition to approximate the off-diagonal blocks. Our main contributions are summarized as follows:

- We develop randomized approximations to matrix-based Rényi’s entropy that transforms the trace estimation into matrix-vector multiplications problem. We extend such strategy to arbitrary values of  $\alpha$  (integer-order and fractional-order) that reduce the overall complexity to roughly  $O(n^2s)$  ( $s$  is the number of Gaussian vectors and  $s \ll n$ ).
- We additionally reveal the intrinsic connection between eigenspectrum estimation and Gram matrix approximation. To this end, we investigate the spectral structure of the Gram matrix and design a novel block low-rank approximation method, which enable us to further reduce the computational burden to  $O(n^2/c + nck)$  ( $c, k \ll n$ ), where  $c$  is the number of clusters and  $k$  denotes the order of rank.
- Theoretically, we provide theoretical accuracy guarantees for each approximator above, and illustrate the properties or connections between them.
- We evaluate the effectiveness of the proposed algorithms on large-scale simulation and real-world datasets, showing remarkable accelerating on various information related tasks.

## 2 Preliminaries

Entropy measures the uncertainty of a random variable using a single scalar quantity [Klir and Wierman, 2013]. For a continuous random variable  $X$  with PDF  $p(\mathbf{x})$  in a finite set  $\mathcal{X}$ , the  $\alpha$ -entropy ( $\alpha > 0, \alpha \neq 1$ )  $\mathbf{H}_\alpha(X)$  is defined by

$$\mathbf{H}_\alpha(X) = \frac{1}{1 - \alpha} \log \int_{\mathcal{X}} p^\alpha(\mathbf{x}) d\mathbf{x} \quad (1)$$

The limit case of Eq. (1) for  $\alpha \rightarrow 1$  yields the well known Shannon’s entropy, i.e.  $\mathbf{H}(X) = - \int_{\mathcal{X}} p(\mathbf{x}) \log p(\mathbf{x}) d\mathbf{x}$ . It is easy to see that Rényi’s entropy is a natural extension of Shannon entropy by introducing a hyper-parameter  $\alpha$ . In real-world applications, the choice of  $\alpha$  is task-specific. On the one hand,  $\alpha$  should be less than 2 even 1 when the learning task requires estimating tails of the distribution or multiple modalities. On the other hand,  $\alpha$  is suggested to be greater than 2 to emphasize mode behavior when we aim to characterize the mean behavior [Principe, 2010, Yu et al., 2019].

It is worth noting that calculating Rényi  $\alpha$ -order entropy requires the prior about the PDF of data, which prevents its more widespread adoption in data-driven science. To alleviate this issue, an alternative measure, namely the matrix-based Rényi’s  $\alpha$ -order entropy was proposed [Giraldo et al., 2014], which resembles quantum Rényi’s entropy in terms of the eigenspectrum of a normalized Hermitian matrix of the projected data in RKHS. It is defined as:

**Definition 1** Let  $\kappa : \mathcal{X} \times \mathcal{X} \mapsto \mathbb{R}$  be a real valued positive kernel that is also infinitely divisible [Bhatia, 2006]. Given  $\{\mathbf{x}_i\}_{i=1}^n \subset \mathcal{X}$ , each  $\mathbf{x}_i$  being a real-valued scalar or vector, and the Gram matrix  $K$  obtained from  $K_{ij} = \kappa(\mathbf{x}_i, \mathbf{x}_j)$ , a matrix-based analogue to Rényi’s  $\alpha$ -entropy can be defined as:

$$\mathbf{S}_\alpha(G) = \frac{1}{1 - \alpha} \log_2(\text{tr}(G^\alpha)) = \frac{1}{1 - \alpha} \log_2 \left[ \sum_{i=1}^n \lambda_i^\alpha(G) \right], \quad (2)$$

where  $G_{ij} = \frac{1}{n} \frac{K_{ij}}{\sqrt{K_{ii}K_{jj}}}$  is a normalized kernel matrix and  $\lambda_i(G)$  denotes the  $i$ -th eigenvalue of  $G$ .

Let  $\Delta_n^+$  be the set of positive definite matrices of size  $n \times n$  whose elements take real values. Then we know from [Giraldo et al., 2014] that  $\mathbf{S}_\alpha(PGP^*) = \mathbf{S}_\alpha(G)$  for any orthonormal matrix  $P$ , and  $\mathbf{S}_\alpha(\frac{1}{n}I) = \log_2(n)$  for identity matrix  $I \in \Delta_n^+$ . Moreover,  $\mathbf{S}_\alpha(G) \leq \mathbf{S}_\alpha(\frac{1}{n}I)$  for  $\alpha > 1$ .

**Definition 2** Given a collection of  $n$  samples  $\{\mathbf{s}_i = (\mathbf{x}_i^1, \mathbf{x}_i^2, \dots, \mathbf{x}_i^L)\}_{i=1}^n$ , each sample contains  $L$  ( $L \geq 2$ ) measurements  $\mathbf{x}^1 \in \mathcal{X}^1, \mathbf{x}^2 \in \mathcal{X}^2, \dots, \mathbf{x}^L \in \mathcal{X}^L$  obtained from the same realization, and the positive definite kernels  $\kappa_1 : \mathcal{X}^1 \times \mathcal{X}^1 \mapsto \mathbb{R}, \kappa_2 : \mathcal{X}^2 \times \mathcal{X}^2 \mapsto \mathbb{R}, \dots, \kappa_L : \mathcal{X}^L \times \mathcal{X}^L \mapsto \mathbb{R}$ , a matrix-based analogue to Rényi's  $\alpha$ -order joint-entropy among  $L$  variables can be defined as:

$$\mathbf{S}_\alpha(G^1, G^2, \dots, G^L) = \mathbf{S}_\alpha \left( \frac{G^1 \circ G^2 \circ \dots \circ G^L}{\text{tr}(G^1 \circ G^2 \circ \dots \circ G^L)} \right), \quad (3)$$

where  $(G^1)_{ij} = \kappa_1(\mathbf{x}_i^1, \mathbf{x}_j^1), (G^2)_{ij} = \kappa_2(\mathbf{x}_i^2, \mathbf{x}_j^2), \dots, (G^L)_{ij} = \kappa_L(\mathbf{x}_i^L, \mathbf{x}_j^L)$ , and  $\circ$  denotes the Hadamard product.

Given Eqs. (2) and (3), the matrix-based Rényi's  $\alpha$ -order mutual information  $I_\alpha(G^i; G^j)$  between variables  $\mathbf{x}^i$  and  $\mathbf{x}^j$  and total correlation  $T_\alpha(\mathbf{x})$  amongst  $\mathbf{x}^1, \mathbf{x}^2, \dots, \mathbf{x}^L$  in analogy of Shannon's mutual information are given by:

$$I_\alpha(G^i; G^j) = S_\alpha(G^i) + S_\alpha(G^j) - S_\alpha(G^i, G^j). \quad (4)$$

$$T_\alpha(\mathbf{x}) = \left[ \sum_{i=1}^L S_\alpha(G^i) \right] - S_\alpha(G^1, G^2, \dots, G^L), \quad (5)$$

As can be seen, the matrix-based entropy functional estimators are independent of the specific dimensions of  $\mathbf{x}^1, \mathbf{x}^2, \dots, \mathbf{x}^L$  and avoid estimation of the underlying data distributions, which makes them suitable to be applied on data with either discrete or continuous distributions. Moreover, it is simple to verify that both  $I_\alpha(G^i; G^j)$  and  $T_\alpha(\mathbf{x})$  are permutation invariant to the ordering of variables.

### 3 Approximating Matrix-based Rényi's Entropy

In this section, we present computationally efficient approaches with statistical guarantees for approximating matrix-based Rényi's entropy. Our general idea is to approximate  $\text{tr}(G^\alpha)$  from two perspectives: 1) approximating the trace operator by random approximation for arbitrary values of  $\alpha$  in cases of both integer and fractional; and 2) approximating the Gram matrix  $G$ . Detailed proofs are provided in Section 4.

#### 3.1 Randomized Approximation

Inspired by the work on randomized trace estimation [Avron and Toledo, 2011], we adopt random algorithms for calculating the matrix-based Rényi's entropy. The following lemma [Boutsidis et al., 2017] characterizes an algorithm that approximates the trace of any symmetric positive semi-definite (PSD) matrix by computing inner products of the matrix with Gaussian random vectors.

**Lemma 1** Let  $G \in \mathbb{R}^{n \times n}$  be a symmetric positive semi-definite matrix. If  $\mathbf{g}_1, \mathbf{g}_2, \dots, \mathbf{g}_s \in \mathbb{R}^n$  are independent random standard Gaussian vectors, then for  $s = \lceil 20 \ln(2/\delta)/\epsilon^2 \rceil$ , with probability at least  $1 - \delta$ ,

$$\left| \text{tr}(G) - \frac{1}{s} \sum_{i=1}^s \mathbf{g}_i^\top G \mathbf{g}_i \right| \leq \epsilon \cdot \text{tr}(G).$$

Lemma 1 immediately implies Algorithm 1 for estimating matrix-based Rényi's entropy for integer  $\alpha$  orders.

---

#### Algorithm 1 Integer order matrix-based Rényi's entropy estimation

---

- 1: **Input:** Kernel matrix  $G \in \mathbb{R}^{n \times n}$ , number of random vectors  $s$ , integer order  $\alpha \geq 2$ .
  - 2: **Output:** Approximation to  $S_\alpha(G)$ .
  - 3: Generate  $s$  independent random standard Gaussian vectors  $\mathbf{g}_i, i = 1, \dots, s$ .
  - 4: **Return:**  $\tilde{\mathbf{S}}_\alpha(G) = \frac{1}{1-\alpha} \log_2 \left( \frac{1}{s} \sum_{i=1}^s \mathbf{g}_i^\top G^\alpha \mathbf{g}_i \right)$ .
-

Indeed, conventional eigenvalue-based approaches calculating the matrix-based Rényi's entropy usually cost  $O(n^3)$  in time complexity. Algorithm 1 seeks for an approximation via matrix-vector multiplications, which costs only  $O(\alpha s \cdot \mathbf{nnz}(G))$  ( $s \ll n$ ), where  $\mathbf{nnz}(G)$  denotes the number of non-zero elements in  $G$  ( $\mathbf{nnz}(G) \approx n^2$  when  $G$  is dense). Theorem 1 provides the quality-of-approximation result for Algorithm 1.

**Theorem 1** *Let  $G \in \mathbb{R}^{n \times n}$  be a normalized PSD kernel matrix and  $\tilde{\mathbf{S}}_\alpha(G)$  be the output of Algorithm 1 with  $s = \lceil 20 \ln(2/\delta)/\epsilon^2 \rceil$ . Then with confidence at least  $1 - \delta$ ,*

$$\left| \mathbf{S}_\alpha(G) - \tilde{\mathbf{S}}_\alpha(G) \right| \leq \left| \frac{1}{\alpha - 1} \right| \log_2(\epsilon + 1).$$

**Remark 1** *Theorem 1 implies that Rényi's entropy could be approximated by matrix-vector multiplication operations, leading substantially lower computational cost than eigenvalue-base methods. The approximation quality depends on the number of queried random vectors  $s$  and hyper-parameter  $\alpha$ . In particular, with the increase of  $\alpha$ , the approximation error decreases for  $\alpha > 1$  and increases otherwise.*

### 3.2 Taylor Series Approximation

Note that the above approach could only handle integer powers of the kernel matrix. For fractional  $\alpha$  cases, it cannot be directly calculated in the same manner. To address this issue, we apply a Taylor series expansion to approximate the fractional power term. The implementing details are presented in Algorithm 2, where the power iteration algorithm 5 [Boutsidis et al., 2017] is used to estimate  $\mu$ , the largest eigenvalue of  $G$ . As can be seen, it only involves matrix-vector multiplications, and the whole computational complexity becomes  $O(ms \cdot \mathbf{nnz}(G))$ .

---

**Algorithm 2** Fractional order matrix-based Rényi's entropy estimation via Taylor series

---

- 1: **Input:** Kernel matrix  $G \in \mathbb{R}^{n \times n}$ , number of random vectors  $s$ , fractional order  $\alpha > 0$ , polynomial order  $m > \alpha$ , eigenvalue upper bound  $\mu$ .
- 2: **Output:** Approximation to  $S_\alpha(G)$ .
- 3: Generate  $s$  independent random standard Gaussian vectors  $\mathbf{g}_i, i = 1, \dots, s$ .
- 4: **Return:**

$$\tilde{\mathbf{S}}_\alpha(G) = \frac{1}{1 - \alpha} \log_2 \frac{\mu^\alpha}{s} \cdot \sum_{i=1}^s \sum_{n=0}^m \binom{\alpha}{n} \mathbf{g}_i^\top \left( \frac{G}{\mu} - I_n \right)^n \mathbf{g}_i.$$


---

The following Theorem states the main quality-of-approximation result for Algorithm 2.

**Theorem 2** *Let  $G \in \mathbb{R}^{n \times n}$  be a normalized PSD kernel matrix and  $\tilde{\mathbf{S}}_\alpha(G)$  be the output of Algorithm 2 with  $s = \lceil 20 \ln(2/\delta)/\epsilon^2 \rceil$  and*

$$m \geq \alpha + \begin{cases} W_0(\beta \sqrt{\frac{(1+\epsilon)\Gamma(\alpha+1)}{\epsilon\pi}})/\beta & \text{if } \lambda_{\min} > 0 \\ \sqrt{\frac{(1+\epsilon)\Gamma(\alpha+1)}{\epsilon\pi}} & \text{if } \lambda_{\min} = 0 \end{cases}.$$

*Then with confidence at least  $1 - \delta$ ,*

$$\left| \mathbf{S}_\alpha(G) - \tilde{\mathbf{S}}_\alpha(G) \right| \leq \left| \frac{1}{1 - \alpha} \right| \log_2(2\epsilon + 1),$$

*where  $\beta = -\log(1 - \lambda_{\min}/\mu)/(\alpha + 1)$ ,  $\lambda_{\min}$  is the smallest eigenvalue of  $G$ , and  $W_0$  is the principal branch of Lambert  $W$  function.*

**Remark 2** *Theorem 2 implies that the approximation error relies on the  $\lambda_{\min}$ ,  $\lambda_{\max}$  and the degree of Taylor series  $m$ . The minimum requirement on the degree of the Taylor series is provided. It can be observed that the approximation error decays with the increase of  $m$ . In particular, when  $\lambda_{\min} \rightarrow \mu$ , the Taylor series approximation is still consistent even for the limited case  $m = 1$ .*

### 3.3 Chebyshev Series Approximation

Chebyshev series provides another way to approximate the fractional power term. It leverages orthogonal polynomials to approximate analytic function. Let  $T_k(x) = \cos(k \arccos(2x/\mu - 1))$  with  $x \in [0, \mu]$  be the Chebyshev polynomials

of the first kind for any integer  $k \geq 0$ , and let  $f_m(x) = c_0 T_0(x)/2 + \sum_{k=1}^m c_k T_k(x)$  with

$$c_k = \frac{2\mu^\alpha \Gamma(\alpha + 1/2)(\alpha)_k}{\sqrt{\pi} \Gamma(\alpha + 1)(\alpha + k)_k},$$

where  $(\alpha)_k = \alpha \cdot (\alpha - 1) \cdots (\alpha - k + 1)$  is the falling factorial and  $\mu$  is an upper bound estimation for the eigenvalues of  $G$ . Algorithm 3 summarizes the procedures on approximating fractional order of matrix-based Rényi's entropy, in which Clenshaw's algorithm [Clenshaw, 1955] is employed to calculate  $F_i(G) = \mathbf{g}_i^\top f_m(G) \mathbf{g}_i$ .

---

**Algorithm 3** fractional order matrix-based Rényi's entropy estimation via Chebyshev series
 

---

- 1: **Input:** Kernel matrix  $G \in \mathbb{R}^{n \times n}$ , number of random vectors  $s$ , fractional order  $\alpha > 0$ , polynomial order  $m > \alpha$ , eigenvalue upper bound  $\mu$ .
- 2: **Output:** Approximation to  $S_\alpha(G)$ .
- 3: Calculate Chebyshev coefficients by:

$$c_k = \frac{2\mu^\alpha \Gamma(\alpha + 1/2)(\alpha)_k}{\sqrt{\pi} \Gamma(\alpha + 1)(\alpha + k)_k}, k = 0, \dots, m.$$

- 4: Generate  $s$  independent random standard Gaussian vectors  $\mathbf{g}_i, i = 1, \dots, s$ .
  - 5: **for**  $i = 1, 2, \dots, s$  **do**
  - 6:     Set  $\mathbf{y}_{m+2} = \mathbf{y}_{m+1} = \mathbf{0}$ .
  - 7:     **for**  $k = m, m - 1, \dots, 0$  **do**
  - 8:          $\mathbf{y}_k = c_k \mathbf{g}_i + 4G\mathbf{y}_{k+1}/\mu - 2\mathbf{y}_{k+1} - \mathbf{y}_{k+2}$ .
  - 9:     **end for**
  - 10:     Calculate  $F_i(G) = c_0 \mathbf{g}_i^\top \mathbf{g}_i/4 + \mathbf{g}_i^\top (\mathbf{y}_0 - \mathbf{y}_2)/2$ .
  - 11: **end for**
  - 12: **Retrun:**  $\tilde{\mathbf{S}}_\alpha(G) = \frac{1}{1-\alpha} \log_2 \left( \frac{1}{s} \sum_{i=1}^s F_i(G) \right)$ .
- 

We establish the following quality-of-approximation guarantee for Algorithm 3.

**Theorem 3** Let  $G \in \mathbb{R}^{n \times n}$  be a normalized PSD kernel matrix and  $\tilde{\mathbf{S}}_\alpha(G)$  be the output of Algorithm 3 with  $s = \lceil 20 \ln(2/\delta)/\epsilon^2 \rceil$  and

$$m \geq \alpha + \begin{cases} \sqrt{\frac{\mu}{\lambda_{\min}}} 2\alpha \sqrt{\frac{\Gamma(\alpha + \frac{1}{2})\Gamma(\alpha)}{\epsilon\pi^{3/2}}} & \text{if } \lambda_{\min} > 0 \\ \sqrt{\frac{\mu}{\lambda_{\max}}} 2\alpha \sqrt{\frac{n\Gamma(\alpha + \frac{1}{2})\Gamma(\alpha)}{\epsilon\pi^{3/2}}} & \text{if } \lambda_{\min} = 0 \end{cases}.$$

Then with confidence at least  $1 - \delta$ ,

$$\left| \mathbf{S}_\alpha(G) - \tilde{\mathbf{S}}_\alpha(G) \right| \leq \left| \frac{1}{1-\alpha} \right| \log_2(3\epsilon + 1),$$

where  $\lambda_{\min}$  and  $\lambda_{\max}$  are the smallest and largest eigenvalue of  $G$  respectively.

**Remark 3** We can draw similar conclusions with Theorem 2, with the only difference being that the number of terms  $m$  required in polynomial approximation to achieve desired accuracy are varying. Specifically, there are two important aspects to highlight:

- In Theorem 2 we take the square root of  $\alpha$ , while in Theorem 3 it is of  $2\alpha$ . This suggests that comparatively fewer terms are needed by the Chebyshev approach when  $\alpha$  is large.
- When  $\lambda_{\min} > 0$ , i.e. the kernel matrix  $G$  is strictly positive definite,  $m$  is growing with  $1/\epsilon$  logarithmically in Theorem 2 but polynomially in Theorem 3. This indicates that the Taylor series achieves better theoretical guarantee than Chebyshev series.

### 3.4 Block Low-Rank Kernel Approximation

In previous analysis, we can conclude that the main computation cost of algorithms above come from matrix-vector multiplications required in both power iteration and trace estimation. The number of arithmetic operations in matrix-vector multiplication is proportional to the density of kernel matrix, i.e. the number of non-zero elements. Considering that the kernel matrix is usually dense in practice, each matrix-vector multiplication still costs  $\mathcal{O}(n^2)$  operations, which

is unaffordable for large matrices. Hence we expect to take full advantage of the structure of the kernel matrix to further reduce the computation burden.

To this end, we first establish the connection between the entropy approximation and the kernel matrix approximation in the following theorem.

**Theorem 4** *For any symmetric PSD matrix  $G$  and its approximation  $\tilde{G}$ , the matrix-based Rényi's  $\alpha$ -order entropy of  $\tilde{G}$  is bounded by*

$$\left| \mathbf{S}_\alpha(G) - \mathbf{S}_\alpha(\tilde{G}) \right| \leq \left| \frac{\alpha}{1-\alpha} \right| \log_2(\sqrt{n} \|G^{-1}\|_2 \|G - \tilde{G}\|_2 + 1).$$

Motivated by the recent progress on kernel approximation [Si et al., 2017], we consider leveraging both the clustering and low-rank structure of kernel matrices. Taking shift-invariant kernel matrices as an example, we first rewrite these kernels as  $\kappa(\mathbf{x}_i, \mathbf{x}_j) = g(\sigma(\mathbf{x}_i - \mathbf{x}_j))$ , where  $g : \mathbb{R}^d \rightarrow \mathbb{R}$  is a measurable function and  $\sigma$  is the scale parameter. Suppose that there exists a appropriate partition  $\mathcal{V}_1, \dots, \mathcal{V}_c$  for the given samples, where each  $\mathcal{V}_s \subset \{1, 2, \dots, n\}$  and  $\mathcal{V}_s \cap \mathcal{V}_t = \emptyset$  for any  $1 \leq s, t \leq c, s \neq t$ . On the one hand, the off-diagonal blocks become quite small for sufficiently large  $\sigma$ . In such cases, the majority of information is stored in the diagonal blocks. It is natural to use block approximation to replace the whole kernel matrices. On the other hand, for a relatively small  $\sigma$ , the impacts of off-diagonal blocks cannot be ignored since the kernel matrix remains dense. To approximate these off-diagonal blocks, we employ a low-rank structure to reduce the computational burden. As a result, the kernel matrix  $G$  can be approximated by  $\tilde{G}$  with block and low rank structure as given in (6).

$$G \approx \tilde{G} = \begin{bmatrix} G^{(1,1)} & G_k^{(1,2)} & \dots & G_k^{(1,c)} \\ G_k^{(2,1)} & G^{(2,2)} & \dots & G_k^{(2,c)} \\ \vdots & \vdots & \ddots & \vdots \\ G_k^{(c,1)} & G_k^{(c,2)} & \dots & G^{(c,c)} \end{bmatrix} \quad (6)$$

where  $G^{(s,s)}$  denotes diagonal blocks and  $G_k^{(s,t)}$  denotes the rank- $k$  approximation for off-diagonal block  $G^{(s,t)}$ . Observing that

$$\|G - \tilde{G}\|_F^2 \leq \sum_{i,j} \kappa(\mathbf{x}_i, \mathbf{x}_j)^2 - \sum_{s=1}^c \sum_{i,j \in \mathcal{V}_s} \kappa(\mathbf{x}_i, \mathbf{x}_j)^2,$$

therefore

$$\min \|G - \tilde{G}\|_F^2 \Leftrightarrow \max \sum_{s=1}^c \sum_{i,j \in \mathcal{V}_s} \kappa(\mathbf{x}_i, \mathbf{x}_j)^2 := D. \quad (7)$$

However, directly maximizing  $D$  can result in all the data being assigned into the same cluster. A common way to solve this problem is to normalize  $D$  by each cluster's size  $|\mathcal{V}_s|$ . This leads to the spectral clustering objective:

$$D^{kernel}(\{\mathcal{V}_s\}_{s=1}^c) = \sum_{s=1}^c \frac{1}{|\mathcal{V}_s|} \sum_{i,j \in \mathcal{V}_s} \kappa(\mathbf{x}_i, \mathbf{x}_j)^2. \quad (8)$$

Optimizing (8) is computational expensive since we have to access all entries in  $G$ . We present a lower bound for  $D^{kernel}(\{\mathcal{V}_s\}_{s=1}^c)$ .

**Theorem 5** *For any shift-invariant Lipschitz continuous kernel function  $\kappa$ ,*

$$D^{kernel}(\{\mathcal{V}_s\}_{s=1}^c) \geq \frac{1}{2n} - R^2 D^{kmeans}(\{\mathcal{V}_s\}_{s=1}^c),$$

where  $R$  is a constant depending on the kernel function, and

$$D^{kmeans}(\{\mathcal{V}_s\}_{s=1}^c) \equiv \sum_{s=1}^c \frac{1}{|\mathcal{V}_s|} \sum_{i,j \in \mathcal{V}_s} \|x_i - x_j\|_2^2$$

is the  $k$ -means objective function.

Theorem 5 suggests that the  $k$ -means algorithm is an ideal choice for selecting the partition  $\mathcal{V}_1, \dots, \mathcal{V}_c$ . We then summarize the block low-rank kernel approximations in Algorithm 4, where the  $k$  largest singular values and the corresponding singular vectors are calculated by Randomized SVD algorithm [Halko et al., 2011]. It takes  $\mathcal{O}(n_r n_c k)$

---

**Algorithm 4** Block Low-Rank Kernel Matrix Approximation
 

---

- 1: **Input:** Shift-invariant kernel matrix  $G \in \mathbb{R}^{n \times n}$ , rank  $k$ , number of clusters  $c$ .
  - 2: **Output:** Approximation to  $G$ .
  - 3: Obtain a partition  $\mathcal{V}_1, \dots, \mathcal{V}_c$  by the  $k$ -means algorithm with  $c$  clusters.
  - 4: Rearrange the kernel matrix  $G$  as a block matrix by the partition  $\mathcal{V}_1, \dots, \mathcal{V}_c$ .
  - 5: Obtain the best rank- $k$  approximation of each off-diagonal block.
  - 6: **Return:** Construct  $\tilde{G}$  by (6).
- 

arithmetic operations for a  $n_r \times n_c$  sub-matrix. Therefore, the overall computational complexity is reduced to  $\mathcal{O}(\frac{n^2}{c} + nck)$ .

The following proposition gives the error bound for block low-rank kernel matrix approximation:

**Proposition 1** *Given samples  $\{\mathbf{x}_i\}_{i=1}^n \subset \mathbb{R}^d$  with a partition  $\mathcal{V}_1, \dots, \mathcal{V}_c$ . Let  $\tilde{G}$  be the output of Algorithm 4 and let the radius of partition  $\mathcal{V}_i$  be  $r_i$  for  $1 \leq i \leq c$ . Assuming  $r_1 \leq r_2 \leq \dots \leq r_c$ , then for any shift-invariant Lipschitz continuous kernel function, we have*

$$\|G - \tilde{G}\|_F \leq 4Lk^{-\frac{1}{d}}\sqrt{2r} \quad (9)$$

where  $L$  is the Lipschitz constant of the kernel function, and  $r = \sum_{i=1}^c r_i^2 |\mathcal{V}_i| \sum_{j=i+1}^c |\mathcal{V}_j|$ .

Combing Theorem 4 and Proposition 1 together yields the following corollary:

**Corollary 1** *Under the same conditions in Proposition 1, the approximation error of  $\mathbf{S}_\alpha(G)$  is bounded by*

$$\left| \mathbf{S}_\alpha(G) - \mathbf{S}_\alpha(\tilde{G}) \right| \leq \left| \frac{\alpha}{1-\alpha} \right| \log_2(\sqrt{n}4Lk^{-\frac{1}{d}} \cdot \sqrt{2r}\|G^{-1}\|_2 + 1).$$

**Remark 4** *Note that there is a trade-off for the choice of  $k$  and  $c$  between time complexity and approximation error. On one hand, selecting a small  $k$  or  $c$  may cause large approximation error, or even worse that the approximated kernel matrix loses its positive semi-definite property. On the other hand, block low-rank approximation may lose its benefits in terms of running time for large  $k$  or  $c$ . In practice, we suggest xxx*

### 3.5 Approximation for Matrix-based Rényi's $\alpha$ Order Mutual Information and Total Correlation

So far, we have developed random approximations (Taylor and Chebyshev series approximation) and Block + Low-Rank approximation for matrix based Rényi's entropy (i.e., Eq. (2)). These approximation algorithms can be applied straightforwardly to calculate matrix-based Rényi's  $\alpha$  order mutual information (i.e., Eq. (4)) and total correlation (i.e., Eq. (5)). This is just because both quantities are just addition and subtraction of several entropy terms. Note that, mutual information and total correlation are fundamental statistics for downstream machine learning tasks, such as feature selection (ranking) and deep neural network training. Comprehensive experiments in Section 5.2 demonstrate the excellent accelerating effect of the proposed approximation algorithms in real-world machine learning problems.

## 4 Proof of Main Results

### 4.1 Proof of Theorem 2

PROOF. We use the binomial series to build our algorithm, which is the Taylor series for function:

$$(1 + A)^\alpha = \sum_{j=0}^{\infty} \binom{\alpha}{j} A^j. \quad (10)$$

Binomial series converge absolutely for symmetric matrices  $A$  with eigenvalues in  $[-1, 1)$ , for any given  $\alpha > 0$ . Taking  $\mu$  the maximum eigenvalue of  $A$ , the eigenvalues of  $\frac{G}{\mu} - I_j$  now lie in interval  $[-1, 0]$ . Replacing  $A$  in (10) by  $\frac{G}{\mu} - I_j$  yields:

$$G^\alpha = \mu^\alpha \cdot \left(\frac{G}{\mu}\right)^\alpha = \mu^\alpha \sum_{j=0}^{\infty} \binom{\alpha}{j} \left(\frac{G}{\mu} - I_j\right)^j. \quad (11)$$

For convenience, we define  $C = \frac{G}{\mu} - I_j$  and the estimation error can be bounded as:

$$\begin{aligned}
 & \left| \mu^\alpha \sum_{i=1}^s \sum_{j=0}^m \binom{\alpha}{j} \mathbf{g}_i^\top C^j \mathbf{g}_i - \text{tr}(G^\alpha) \right| \\
 & \leq \mu^\alpha \left| \sum_{i=1}^s \sum_{j=0}^m \binom{\alpha}{j} \mathbf{g}_i^\top C^j \mathbf{g}_i - \sum_{j=0}^m \binom{\alpha}{j} \text{tr}(C^j) \right| \\
 & \quad + \mu^\alpha \left| \sum_{j=m+1}^{\infty} \binom{\alpha}{j} \text{tr}(C^j) \right| \\
 & \leq \epsilon \mu^\alpha \left| \sum_{j=0}^m \binom{\alpha}{j} \text{tr}(C^j) \right| + \mu^\alpha \left| \sum_{j=m+1}^{\infty} \binom{\alpha}{j} \text{tr}(C^j) \right| \tag{12}
 \end{aligned}$$

$$\begin{aligned}
 & \leq \epsilon \text{tr}(G^\alpha) + \mu^\alpha (1 + \epsilon) \left| \sum_{j=m+1}^{\infty} \binom{\alpha}{j} \text{tr}(C^j) \right| \\
 & \leq \epsilon \text{tr}(G^\alpha) + \mu^\alpha (1 + \epsilon) \left| \sum_{j=0}^{\infty} \binom{\alpha}{m+1} \binom{\alpha}{j} \text{tr}(C^{m+1} C^j) \right| \tag{13}
 \end{aligned}$$

$$\leq \epsilon \text{tr}(G^\alpha) + (1 + \epsilon) \left| \binom{\alpha}{m+1} \left( \frac{\lambda_{\min}}{\mu} - 1 \right)^{m+1} \text{tr}(G^\alpha) \right| \tag{14}$$

(12) follows by applying Lemma 1 on matrix  $\sum_{j=0}^m \binom{\alpha}{j} C^j$ , with probability at least  $1 - \delta$ . (13) follows by the property of binomial series. (14) follows by the von Neumann's trace inequality, that for any two matrices  $A$  and  $B$ ,  $\text{tr}(AB) \leq \sum_i \lambda_i(A) \lambda_i(B)$ , where  $\lambda_i(A)$  denotes the  $i$ -th eigenvalue of  $A$  (and respectively for  $\lambda_i(B)$ ). Then  $\text{tr}(C^{m+1} C^j) \leq |\lambda_{\min}(C)|^{m+1} \sum_i \lambda_i^j(C) = |\lambda_{\min}/\mu - 1|^{m+1} \text{tr}(C^j)$ , where  $\lambda_{\min}(C) = \lambda_{\min}/\mu - 1$  is the smallest eigenvalue of  $C$ , since all eigenvalues of  $C$  are negative.

We use the following lemma to establish the upper bound of binomial term  $\binom{\alpha}{m}$ :

**Lemma 2** [Das, 2019] Let  $\Gamma(x)$  be the gamma function and let  $R(x, y) = \Gamma(x + y)/\Gamma(x)$ , then

$$\begin{aligned}
 R(x, y) & \geq x^y & \text{for } 1 \leq y \leq 2, \\
 R(x, y) & \geq x(x+1)^{y-1} & \text{for } y \geq 2.
 \end{aligned}$$

By transforming the binomial term into gamma functions, we have the following bound:

$$\begin{aligned}
 \left| \binom{\alpha}{m+1} \right| & = \left| \frac{\Gamma(\alpha+1)}{\Gamma(m+2)\Gamma(\alpha-m)} \right| \\
 & \leq \left| \frac{\Gamma(\alpha+1)}{\Gamma(m-\alpha+1)\Gamma(\alpha-m)} \right| \\
 & \quad \cdot \begin{cases} \frac{1}{(m-\alpha+1)^{\alpha+1}} & 0 < \alpha < 1 \\ \frac{1}{(m-\alpha+1)(m-\alpha+2)^\alpha} & \alpha > 1 \end{cases} \tag{15}
 \end{aligned}$$

$$\begin{aligned}
 & \leq \frac{\Gamma(\alpha+1)}{\pi(m-\alpha+1)} \frac{1}{(m-\alpha+1)^\alpha} \\
 & \leq \frac{\Gamma(\alpha+1)}{\pi(m-\alpha+1)^{\alpha+1}}. \tag{16}
 \end{aligned}$$

(15) follows by applying Lemma 2 on  $R(m-\alpha, \alpha+1)$ . (16) follows by Euler's reflection formula that for any fractional number  $z$ ,  $\Gamma(z)\Gamma(1-z) = \pi/\sin \pi z$ . Finally the criterion for choosing  $m$  could be obtained by solving the following



inequality:

$$(1 + \epsilon) \left| \frac{\lambda_{\min}}{\mu} - 1 \right|^{m+1} \frac{\Gamma(\alpha + 1)}{\pi(m - \alpha + 1)^{\alpha+1}} < \epsilon,$$

$$m \geq \alpha + \begin{cases} W_0(\beta \sqrt[\alpha]{\frac{(1+\epsilon)\Gamma(\alpha+1)}{\epsilon\pi}}) / \beta & \text{if } \beta > 0 \\ \sqrt[\alpha]{\frac{(1+\epsilon)\Gamma(\alpha+1)}{\epsilon\pi}} & \text{if } \beta = 0 \end{cases},$$

where  $\beta = -\log(1 - \lambda_{\min}/\mu)/(\alpha + 1)$ . ■

## 4.2 Proof of Theorem 3

PROOF. Chebyshev series of the first kind is defined as  $T_n(x) = \cos(n \arccos x)$  for  $n \in \mathbb{N}$  on interval  $[-1, 1]$ . Since the eigenvalues of our kernel matrix all lie in  $[0, \mu]$ , the affine transformation

$$F(x) = \frac{\mu}{2}(x + 1), \quad \hat{T}_n(x) = T_n \circ F.$$

allows us to define Chebyshev series on interval  $[0, \mu]$ . The coefficients of Chebyshev series  $\hat{T}_n$  can be calculated by:

$$\begin{aligned} c_n &= \frac{2}{\pi} \int_0^\pi F^\alpha(\cos\theta) \cos(n\theta) d\theta \\ &= \frac{2}{\pi} \int_0^\pi \left( \frac{\mu}{2}(\cos\theta + 1) \right)^\alpha \cos(n\theta) d\theta \\ &= \frac{2\mu^\alpha \Gamma(\alpha + \frac{1}{2})(\alpha)_n}{\sqrt{\pi} \Gamma(\alpha + 1)(\alpha + n)_n}. \end{aligned}$$

where  $(\alpha)_n$  is the falling factorial:  $(\alpha)_n = \alpha \cdot (\alpha - 1) \cdot \dots \cdot (\alpha - n + 1)$ . We now obtain the infinite series expression of the entropy term:

$$\lambda^\alpha = \frac{c_0}{2} + \sum_{i=1}^{\infty} c_i \hat{T}_i(\lambda).$$

We denote  $f_m(x) = c_0 + \sum_{i=1}^m c_i \hat{T}_i(x)$  be the Chebyshev series for convenience, then for each eigenvalue  $\lambda$  of  $G$ :

$$\begin{aligned} |\lambda^\alpha - f_m(\lambda)| &= \left| \sum_{i=m+1}^{\infty} c_i \hat{T}_i(\lambda) \right| \\ &\leq \sum_{i=m+1}^{\infty} |c_i| = \sum_{i=m+1}^{\infty} \left| \frac{2\mu^\alpha \Gamma(\alpha + \frac{1}{2})(\alpha)_i}{\sqrt{\pi} \Gamma(\alpha + 1)(\alpha + i)_i} \right| \end{aligned} \quad (17)$$

$$\begin{aligned} &= \frac{2\mu^\alpha}{\sqrt{\pi}} \sum_{i=m+1}^{\infty} \left| \frac{\Gamma(\alpha + \frac{1}{2})\Gamma(\alpha + 1)}{\Gamma(\alpha + i + 1)\Gamma(\alpha - i + 1)} \right| \\ &\leq \frac{2\mu^\alpha}{\sqrt{\pi}} \sum_{i=m+1}^{\infty} \left| \frac{\Gamma(\alpha + \frac{1}{2})\Gamma(\alpha + 1)}{\Gamma(i - \alpha)\Gamma(\alpha - i + 1)(i - \alpha)^{2\alpha+1}} \right| \end{aligned} \quad (18)$$

$$\leq \frac{2\mu^\alpha \Gamma(\alpha + \frac{1}{2})\Gamma(\alpha + 1)}{\pi^{3/2}} \sum_{i=m+1}^{\infty} \left| \frac{1}{(i - \alpha)^{2\alpha+1}} \right| \quad (19)$$

$$\leq \frac{2\mu^\alpha \Gamma(\alpha + \frac{1}{2})\Gamma(\alpha + 1)}{\pi^{3/2}} \int_m^\infty \frac{1}{(x - \alpha)^{2\alpha+1}} dx \quad (20)$$

$$\begin{aligned} &= \frac{2\mu^\alpha \Gamma(\alpha + \frac{1}{2})\Gamma(\alpha + 1)}{\pi^{3/2}} \frac{1}{2\alpha(m - \alpha)^{2\alpha}} \\ &= \frac{\mu^\alpha \Gamma(\alpha + \frac{1}{2})\Gamma(\alpha)}{\pi^{3/2}(m - \alpha)^{2\alpha}}. \end{aligned}$$

(17) follows by noticing that  $\hat{T}_n(x) \in [-1, 1]$  for any  $x \in [0, \mu]$ . (18) follows by applying Lemma 2 on  $R(i - \alpha, 2\alpha + 1)$  similar to (15). (19) follows by Euler's reflection formula similar to (16). (20) follows by noticing that  $n^{-k} \leq \int_{n-1}^n x^{-k} dx$  for  $n > 1$  and  $k > 1$ .

If  $G$  has full rank, i.e.,  $\lambda_{min} > 0$ , then by choosing  $m$  as:

$$m \geq \alpha + \sqrt{\frac{\mu}{\lambda_{min}}} \sqrt[2\alpha]{\frac{\Gamma(\alpha + \frac{1}{2})\Gamma(\alpha)}{\epsilon\pi^{3/2}}},$$

we have

$$|\lambda^\alpha - f_m(\lambda)| \leq \epsilon\lambda_{min}^\alpha \leq \epsilon\lambda^\alpha.$$

Then the trace of  $G^\alpha$  is bounded as:

$$\begin{aligned} & \left| \sum_{i=1}^s \mathbf{g}_i^\top f_m(G) \mathbf{g}_i - \text{tr}(G^\alpha) \right| \\ & \leq \left| \sum_{i=1}^s \mathbf{g}_i^\top f_m(G) \mathbf{g}_i - \text{tr}(f_m(G)) \right| \\ & \quad + |\text{tr}(f_m(G)) - \text{tr}(G^\alpha)| \\ & \leq \epsilon \cdot \text{tr}(f_m(G)) + |\text{tr}(f_m(G)) - \text{tr}(G^\alpha)| \\ & \leq \epsilon \cdot \text{tr}(G^\alpha) + (1 + \epsilon) \cdot |\text{tr}(f_m(G)) - \text{tr}(G^\alpha)| \\ & \leq \epsilon \cdot \text{tr}(G^\alpha) + (1 + \epsilon) \cdot \sum_{i=1}^n |\lambda_i^\alpha - f_m(\lambda_i)| \\ & \leq \epsilon \cdot \text{tr}(G^\alpha) + \epsilon(1 + \epsilon) \cdot \sum_{i=1}^n \lambda_i^\alpha \\ & \leq 3\epsilon \cdot \text{tr}(G^\alpha). \end{aligned} \tag{21}$$

(21) follows by applying Lemma 1 on matrix  $f_m(G)$ .

Otherwise if  $G$  is rank deficient, i.e.,  $\lambda_{min} = 0$ , then by choosing  $m$  as:

$$m \geq \alpha + \sqrt{\frac{\mu}{\lambda_{max}}} \sqrt[2\alpha]{\frac{n\Gamma(\alpha + \frac{1}{2})\Gamma(\alpha)}{\epsilon\pi^{3/2}}},$$

we have

$$|\lambda^\alpha - f_m(\lambda)| \leq \frac{\epsilon}{n} \lambda_{max}^\alpha.$$

Then the trace of  $G^\alpha$  is bounded as:

$$\begin{aligned} & \left| \sum_{i=1}^s \mathbf{g}_i^\top f_m(G) \mathbf{g}_i - \text{tr}(G^\alpha) \right| \\ & \leq \epsilon \cdot \text{tr}(G^\alpha) + (1 + \epsilon) \cdot \sum_{i=1}^n |\lambda_i^\alpha - f_m(\lambda_i)| \\ & \leq \epsilon \cdot \text{tr}(G^\alpha) + \epsilon(1 + \epsilon) \cdot \lambda_{max}^\alpha \\ & \leq 3\epsilon \cdot \text{tr}(G^\alpha). \end{aligned}$$

■

### 4.3 Proof of Theorem 4

PROOF. Noticing that

$$\begin{aligned}
 \left| \mathbf{S}_\alpha(G) - \mathbf{S}_\alpha(\tilde{G}) \right| &= \left| \frac{1}{1-\alpha} \log_2 \frac{\sum_{i=1}^n \lambda_i^\alpha(\tilde{G})}{\sum_{i=1}^n \lambda_i^\alpha(G)} \right| \\
 &\leq \left| \frac{1}{1-\alpha} \log_2 \max_i \frac{\lambda_i^\alpha(\tilde{G})}{\lambda_i^\alpha(G)} \right| \\
 &= \left| \frac{\alpha}{1-\alpha} \log_2 \max_i \frac{\lambda_i(\tilde{G})}{\lambda_i(G)} \right|. \tag{22}
 \end{aligned}$$

There is no restriction on the order of eigenvalues, i.e. we can reorder the eigenvalues  $\lambda_i(G)$  and  $\lambda_i(\tilde{G})$  arbitrarily for  $i = 1, \dots, n$ . By Corollary 3.3 in [Li and Sun, 2005], there exists a permutation  $\tau$  of  $\{1, \dots, n\}$  such that for normal non-singular matrix  $A$ ,

$$\max \left| \frac{\mu_{\tau(i)} - \lambda_i}{\lambda_i} \right| \leq \sqrt{n(n-s+1)} \|A^{-1}\|_2 \|E\|_2. \tag{23}$$

where  $\lambda_i$  and  $\mu_i$  are eigenvalues of  $A$  and  $\tilde{A} = A + E$  respectively, assuming there exists a unitary matrix  $U$  such that  $U^*AU = \mathbf{diag}(A_1, \dots, A_s)$ , where  $1 \leq s \leq n$ , and  $A_i$  is an upper triangular matrix for  $i = 1, \dots, s$ . When the approximation  $\tilde{G}$  is symmetric,  $\tilde{G}$  is also a normal matrix and  $s = n$  is guaranteed. Combining (22) and (23) yields the result. ■

### 4.4 Proof of Theorem 5

PROOF. For any shift-invariant kernel function, there exists a real valued function  $f \in \mathbb{R}^d \mapsto \mathbb{R}$  so that for any data points  $\mathbf{x}_i, \mathbf{x}_j \in \mathbb{R}^d$ ,

$$\kappa(\mathbf{x}_i, \mathbf{x}_j) = f(\mathbf{x}_i - \mathbf{x}_j) \geq f(\mathbf{0}) - L\|\mathbf{x}_i - \mathbf{x}_j\|_2,$$

where  $L$  is the Lipschitz constant of  $f(\cdot)$ . Then the elements of matrix  $G$  satisfies:

$$\begin{aligned}
 G_{ij} &= \frac{1}{n} \frac{\kappa(\mathbf{x}_i, \mathbf{x}_j)}{\sqrt{\kappa(\mathbf{x}_i, \mathbf{x}_i)\kappa(\mathbf{x}_j, \mathbf{x}_j)}} = \frac{f(\mathbf{x}_i - \mathbf{x}_j)}{nf(\mathbf{0})} \\
 &\geq \frac{1}{nf(\mathbf{0})} (f(\mathbf{0}) - L\|\mathbf{x}_i - \mathbf{x}_j\|_2) \\
 &= \frac{1}{n} - \frac{L}{nf(\mathbf{0})} \|\mathbf{x}_i - \mathbf{x}_j\|_2.
 \end{aligned}$$

Let  $R \equiv L/nf(\mathbf{0})$ , we have

$$G_{ij} + R\|\mathbf{x}_i - \mathbf{x}_j\|_2 \geq \frac{1}{n}.$$

Taking the square of both sides

$$G_{ij}^2 + R^2\|\mathbf{x}_i - \mathbf{x}_j\|_2^2 + 2G_{ij}R\|\mathbf{x}_i - \mathbf{x}_j\|_2 \geq \frac{1}{n^2}.$$

From the classical arithmetic and geometric mean inequality, we get the following bound:

$$2G_{ij}R\|\mathbf{x}_i - \mathbf{x}_j\|_2 \leq G_{ij}^2 + R^2\|\mathbf{x}_i - \mathbf{x}_j\|_2^2,$$

hence

$$G_{ij}^2 + R^2\|\mathbf{x}_i - \mathbf{x}_j\|_2^2 \geq \frac{1}{2n^2}.$$

According to the definition of  $D^{kernel}$ :

$$\begin{aligned}
 D^{kernel}(\{\mathcal{V}_s\}_{s=1}^c) &= \sum_{s=1}^c \frac{1}{|\mathcal{V}_s|} \sum_{i,j \in \mathcal{V}_s} G_{ij}^2 \\
 &\geq \sum_{s=1}^c \frac{1}{|\mathcal{V}_s|} \sum_{i,j \in \mathcal{V}_s} \left( \frac{1}{2n^2} - R^2 \|\mathbf{x}_i - \mathbf{x}_j\|_2^2 \right) \\
 &= \frac{1}{2n} - R^2 \sum_{s=1}^c \frac{1}{|\mathcal{V}_s|} \sum_{i,j \in \mathcal{V}_s} \|\mathbf{x}_i - \mathbf{x}_j\|_2^2 \\
 &= \frac{1}{2n} - R^2 D^{kmeans}(\{\mathcal{V}_s\}_{s=1}^c).
 \end{aligned}$$

This completes the proof. ■

#### 4.5 Proof of Proposition 1

PROOF. Denote  $G^{(s,t)}$  as one block of matrix  $G$  with rows  $\mathcal{V}_s$  and columns  $\mathcal{V}_t$ . By Theorem 2 in [Si et al., 2017], for any shift-invariant Lipschitz continuous kernel function with Lipschitz constant  $L$ , we have the following bound:

$$\|G^{(s,t)} - G_k^{(s,t)}\|_F \leq 4Lk^{-\frac{1}{d}} \sqrt{|\mathcal{V}_s||\mathcal{V}_t|} \min(r_s, r_t).$$

Summing up the inequality above for all off-diagonal blocks yields the final result:

$$\begin{aligned}
 \|G - \tilde{G}\|_F &= \sqrt{\sum_{s,t=1 \dots c, s < t} 2\|G^{(s,t)} - G_k^{(s,t)}\|_F^2} \\
 &\leq 4Lk^{-\frac{1}{d}} \sqrt{\sum_{s,t=1 \dots c, s < t} 2|\mathcal{V}_s||\mathcal{V}_t| \min^2(r_s, r_t)} \\
 &= 4Lk^{-\frac{1}{d}} \sqrt{2 \sum_{i=1}^c r_i^2 |\mathcal{V}_i| \sum_{j=i+1}^c |\mathcal{V}_j|}.
 \end{aligned}$$

■

## 5 Experimental Results

We evaluate the performance of the proposed approximation algorithms on large-scale simulation and real-world data. All numerical studies are conducted with an Intel i7-10700 (2.90GHz) CPU, an RTX 2080Ti GPU and 64GB of RAM. Approximation algorithms are implemented both in C++ and Python, with k-means algorithm provided by OpenCV [Bradski, 2000], and fundamental linear algebra functions provided by Eigen [Guennebaud et al., 2010] and Pytorch [Paszke et al., 2019] respectively.

### 5.1 Simulation Studies

In our experiments, the simulation data are generated by mixture of Gaussian distribution  $\frac{1}{2}N(-1, \mathbf{I}_d) + \frac{1}{2}N(1, \mathbf{I}_d)$  with  $n = 10,000$  and  $d = 10$ , the size of the kernel matrix is then  $10,000 \times 10,000$ . We choose Gaussian kernel  $\kappa(\mathbf{x}_i, \mathbf{x}_j) = \exp(-\|\mathbf{x}_i - \mathbf{x}_j\|_2^2 / 2\sigma^2)$  with  $\sigma = 1$  for calculating matrix-based Rényi's entropy. We set order of rank  $k = 80$  and number of clusters  $c = 20$  in block low-rank approximation experiments. To reduce the impact of randomness, we run each test for  $K = 100$  times and report the mean relative error (MRE) and corresponding standard deviation (SD). The oracle  $\mathbf{S}_\alpha(G)$  is computed through the trivial  $\mathcal{O}(n^3)$  eigenvalue approach. We use the high resolution clock provided by the C++ standard library, whose precision reaches nanoseconds.

#### 5.1.1 Randomized Approximation

We examine the performance of the trace estimation algorithm ‘‘Trace’’ and its combination with block low-rank approximation ‘‘Trace + Low-rank’’ for Rényi's entropy with integer orders. Algorithm 1 is implemented with

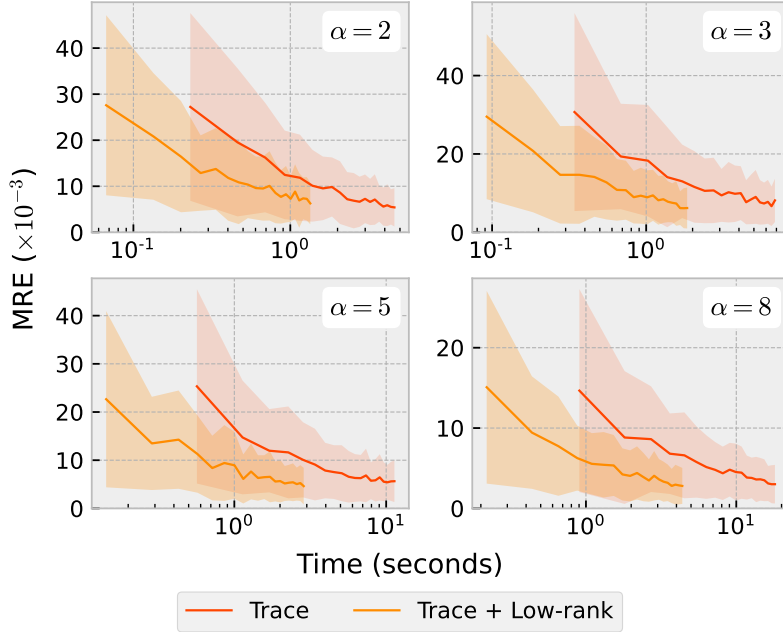


Figure 1: Time vs. MRE curves for integer  $\alpha$ -order Rényi's entropy estimation.

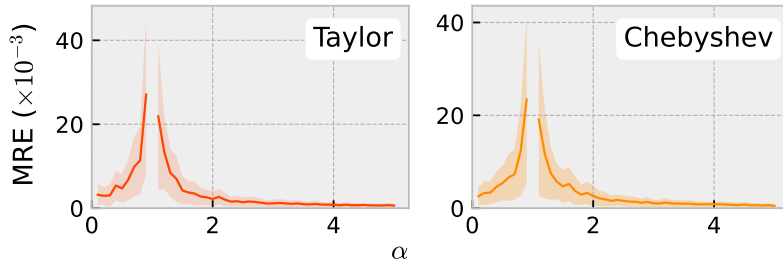


Figure 2:  $\alpha$  vs. MRE curves for fractional  $\alpha$ -order algorithms.

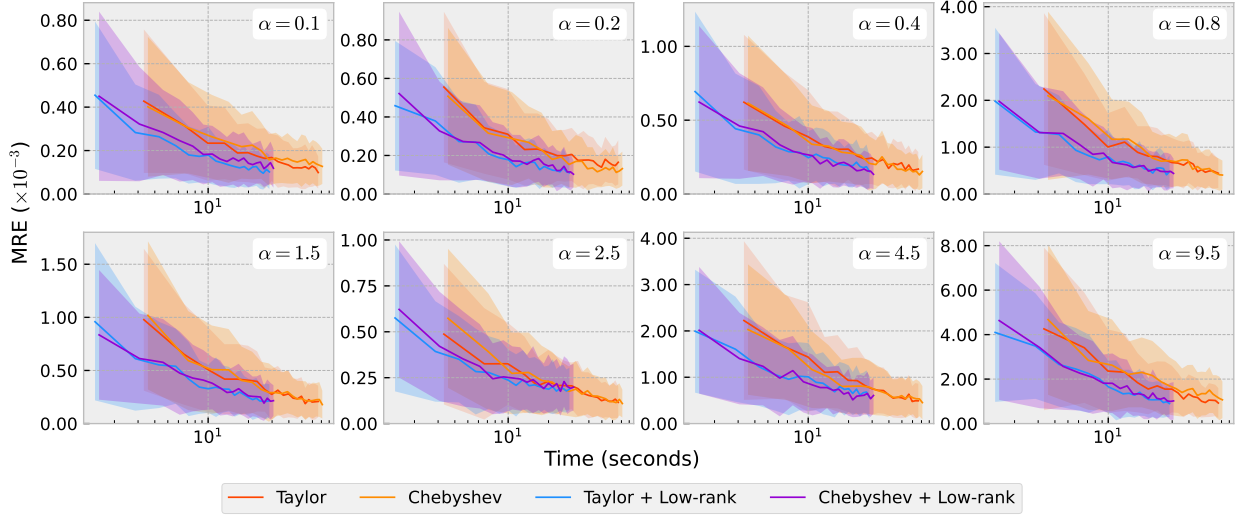
$\alpha \in \{2, 3, 5, 8\}$ . The number of random Gaussian vectors  $s$  ranges from 20 to 200 in increments of 20. The Time vs. MRE curves for different  $\alpha$  are shown in Figure 1, in which the shaded area indicates corresponding SD. We observe that when  $s$  is large enough, “Trace + Low-rank” runs faster than “Trace” while yielding comparable estimation error.

### 5.1.2 Taylor & Chebyshev Series Approximation

We further evaluate the approximation effect for fractional  $\alpha$  orders. The results on describing the impact of  $\alpha$  for Taylor series and Chebyshev series approximations are reported in Figure 2. We can see that the approximation error grows with the increase of  $\alpha$  for  $\alpha < 1$  and decreases otherwise. This phenomenon supports our claims in Theorem 2 and 3, where the term  $|\frac{1}{1-\alpha}|$  dominates the approximation error.

Moreover, we test Algorithms 2 and 3 with or without block low-rank kernel approximation by setting the number of terms  $m = 30$  in polynomial series. Again, the number of random Gaussian vectors  $s$  ranges from 20 to 200 in increments of 20. The results are shown in Figure 3 and Table 1. It can be observed that the Chebyshev methods runs slightly slower than Taylor. For a large range of different  $\alpha$ , Taylor and Chebyshev approaches produces similar MRE. Besides, the block low-rank methods save more than half of running time while only introducing negligible error in approximation.

Next we demonstrate that the proposed algorithms are applicable to different kinds of kernel functions. Considering the prerequisite that matrix based Rényi's entropy supports only infinitely divisible kernels, we choose the following widely-used ones to constitute our benchmark:


 Figure 3: Time vs. MRE curves for fractional  $\alpha$ -order Rényi's entropy estimation with  $m = 30$ .

Method	$\alpha$		0.1	0.4	1.5	4.5
	Time (s)		0.2	0.8	2.5	9.5
Eigenvalue	219.8		-	-	-	-
Taylor	66.3		$0.099 \pm 0.074$	$0.160 \pm 0.119$	$0.187 \pm 0.148$	$0.491 \pm 0.370$
Chebyshev	71.1		$0.127 \pm 0.081$	$0.129 \pm 0.102$	$0.179 \pm 0.131$	$0.453 \pm 0.358$
Taylor + Low-rank	28.6		$0.095 \pm 0.075$	$0.152 \pm 0.109$	$0.209 \pm 0.167$	$0.570 \pm 0.459$
Chebyshev + Low-rank	30.7		$0.116 \pm 0.084$	$0.133 \pm 0.099$	$0.192 \pm 0.166$	$0.606 \pm 0.389$

 Table 1: Time and  $(\text{MRE} \pm \text{SD}) \times 10^{-3}$  for fractional  $\alpha$ -order Rényi's entropy estimation with  $m = 30$ ,  $s = 200$ .

- Polynomial kernel:  $\kappa(\mathbf{x}_i, \mathbf{x}_j) = (\mathbf{x}_i^\top \mathbf{x}_j + r)^p$  with  $r = 1$  and  $p = 2, 4$ .
- Gaussian kernel:  $\kappa(\mathbf{x}_i, \mathbf{x}_j) = \exp(-\|\mathbf{x}_i - \mathbf{x}_j\|_2^2 / 2\sigma^2)$  with  $\sigma = 0.5, 1$ .

We set  $\alpha = 1.5$  and  $m = 50$ , while  $s$  ranges from 10 to 100 in increments of 10. For polynomial kernel, we set  $d = 1000$  to prevent too many zero eigenvalues appearing in  $G$ . For Gaussian kernel, we keep the previous settings, and add the corresponding comparisons with low-rank structure due to its shift-invariant property. The evaluation results are presented in Figure 4. It can be seen that for fixed  $\alpha$ ,  $m$  and  $c$ , Taylor and Chebyshev series approximation achieve similar performance. This observation supports the effectiveness of approximating different kernel functions by Taylor and Chebyshev series.

### 5.1.3 Effect of Block Low-rank Approximation

We finally examine the performance of block low-rank kernel approximation with different number of clusters  $c$  and different ranks  $k$ . Our purpose is to demonstrate that our approximations can reach a satisfactory trade-off in a suitable range of both  $c$  and  $k$ , although too small or too large values of  $c$  or  $k$  are not desirable. Additionally, we also wish to provide practitioners some insights on how to appropriately select the most suitable approximation in real applications. We use the Gaussian kernel same as above with  $\alpha = 2.5$ ,  $s = 100$  and  $m = 40$ . To evaluate the impact of  $c$  and  $k$  respectively, we take a grid search for  $c$  varying from 2 to 20 with step 2 and  $k$  varying from 10 to 100 with step 10 using Chebyshev approximation. The results are shown in Figure 5. Obviously, the Chebyshev algorithm with block low-rank kernel approximation yield comparable estimation accuracy to the algorithms without matrix approximation for large  $c$  and  $k$ , while saving nearly half of running time. We also find that the approximation error decreases with the increase of  $c$  in most cases, but with running time decreasing at the same time for small  $c$ . This observation is just due

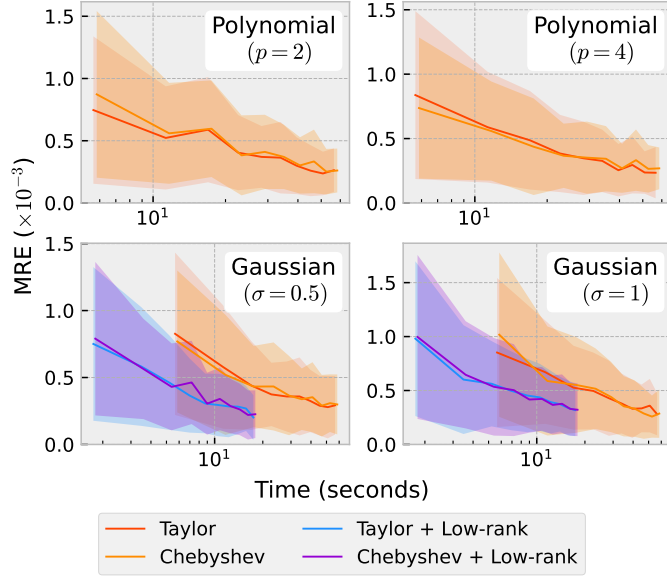
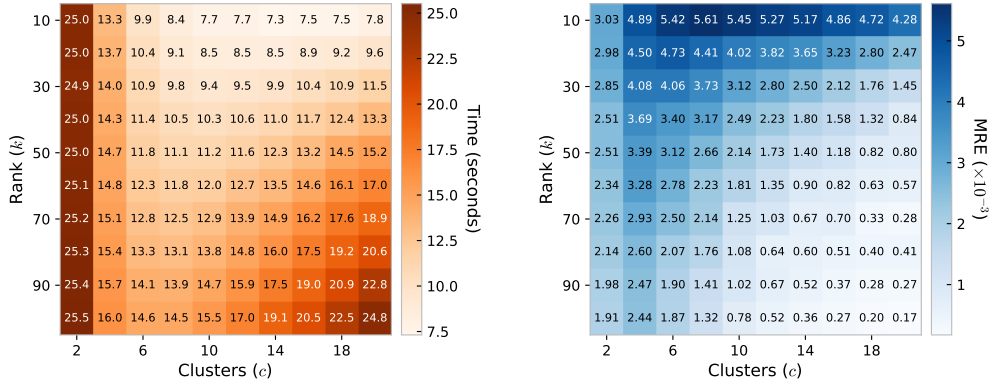


Figure 4: Time vs. MRE curves evaluated on different kernels.


 Figure 5: Impact of  $c$  and  $k$  on Time and MRE in block low-rank kernel approximation. For comparison, the Chebyshev algorithm without low-rank approximation yields  $MRE 0.19 \times 10^{-3}$  in 46.9 seconds.

to the  $\mathcal{O}(\frac{n^2}{c} + nck)$  complexity of the approximated matrix-vector multiplication. In this sense, we recommend a range of  $c$  between 10 and 20. Similarly, a range of  $k$  between 50 and 100 is preferred.

Additionally, we evaluate such combination for a  $50000 \times 50000$  Gram matrix. ‘‘Chebyshev + low-rank’’ approximations take less than 8 minutes to obtain the entropy value, whereas the original estimator requires more than 8 hours. From a practical viewpoint, we suggest using such combination to achieve an ideal effect.

## 5.2 Real-world Data Studies

Following Shannon’s definition of joint entropy and mutual information, corresponding extended information measures defined on matrix-based Rényi’s entropy could be derived accordingly Eqs. (4) and (5). In real-world scenarios, these extended information quantities enable much wider range of applications e.g. feature selection, dimension reduction and information based clustering. In this section, we will show that our approximation algorithms are also well-suited for these extended information measures, and can be directly applied to accomplish complex tasks as well as maintaining the outstanding performance of Rényi’s entropy. In the following experiments, we select Gaussian kernel with  $\sigma = 1$  and  $\alpha = 2$  for simplicity.

Dataset	# Instance	# Feature	# Class	Type
Covid	5434	21	2	D
Optdigits	5620	65	10	D
Statlog	6435	37	6	D
Gesture	11674	65	4	D
Spambase	4601	57	2	C
Waveform	5000	40	3	C
Galaxy	9150	16	2	C
Beans	13611	17	7	C

Table 2: Datasets used in feature selection tasks. Type D is for discrete data and C for continuous.

Method	Dataset								Average Ranking
	Covid	Optdigits	Statlog	Gesture	Spambase	Waveform	Galaxy	Beans	
MIFS [R. Battiti, 1994]	5.96	9.13	13.07	39.67	22.06	25.04	12.85	7.07	5.5
FOU [Brown, 2009]	3.59	14.04	12.32	39.34	19.17	20.34	12.86	7.69	5.0
MIM [Lewis, 1992]	4.31	12.49	13.58	33.70	9.93	20.84	0.74	9.10	5.3
MRMR [Peng et al., 2005]	4.36	9.13	12.91	34.42	9.87	16.66	12.87	8.26	4.1
JMI [Yang, 1999]	4.32	11.01	13.36	39.03	9.98	16.18	0.72	8.96	4.5
CMIM [Fleuret, 2004]	4.4	8.43	13.77	40.30	9.80	17.3	5.98	7.59	4.6
RMI [Yu et al., 2019]	3.86	9.50	13.35	20.28	9.82	19.98	0.51	7.16	2.8
ARMI (Ours)	4.36	8.91	13.36	20.06	10.71	20.98	0.51	7.32	3.8

Table 3: Feature selection results in terms of classification error (%).

### 5.2.1 Mutual Information for Feature Selection

Given a set of features  $S = \{\mathbf{X}_1, \dots, \mathbf{X}_n\}$ , the feature selection task aims to find a smallest subset of  $S$  while trying to maximize the relevance about the labels  $\mathbf{Y}$ . In the view of information theory, our goal is to maximize  $\mathbf{I}(\{\mathbf{X}_{i_1}, \dots, \mathbf{X}_{i_k}\}; \mathbf{Y})$ , where  $i_1, \dots, i_k$  indicate the selected features. However, the curse of high dimension causes this objective extremely hard to estimate. By employing the extension of multivariate matrix-based Rényi’s mutual information [Yu et al., 2019], we are finally granted direct measure to this information quantity. We evaluate the performance of matrix-based Rényi’s mutual information (RMI) and RMI approximated by our algorithms (ARMI) on 8 well-known classification datasets used in previous works [Dua and Graff, 2017, Koklu and Ozkan, 2020, Abolfathi et al., 2018, Yu et al., 2019, Vinh et al., 2016] which cover a wide range of instance-feature ratio, number of classes and data source domains, as shown in Table 2. For completeness, we compare with state-of-the-art information based feature selection methods, including Mutual Information-based Feature Selection (MIFS) [R. Battiti, 1994], First-Order Utility (FOU) [Brown, 2009], Mutual Information Maximization (MIM) [Lewis, 1992], Maximum-Relevance Minimum-Redundancy (MRMR) [Peng et al., 2005], Joint Mutual Information (JMI) [Yang, 1999] and Conditional Mutual Information Maximization (CMIM) [Fleuret, 2004].

In our experiments, continuous features are discretized into 5 bins by equal-width strategy [Vinh et al., 2014] for non-Rényi methods. We choose the Support Vector Machine algorithm implemented by libSVM [Chang and Lin, 2011] with RBF kernel ( $\sigma = 1$ ) as the classifier and employ 10-fold cross validation. In our observation, classification error tends to stop decreasing after incrementally selecting the first  $k = 8$  features (shown in the appendix), so we select the first 8 most informative features step by step through a greedy criterion and report the best validation error achieved by each method. Experiment results are shown in Table 3 in terms of classification error, with corresponding running time reported in Table 5 for RMI and ARMI. As we can see, ARMI achieves 5 to 10 times speedup comparing to original RMI on all datasets while introducing only less than 1% error in classification experiments, which is still significantly lower than other methods in comparison. This demonstrates the great potential of the proposed approximating algorithms in machine learning applications.

### 5.2.2 Mutual Information for Feature Ranking

Feature ranking provides an efficient way to implement feature selection, it aims to identify the most informative features about the label  $\mathbf{Y}$  for the given set  $S = \{\mathbf{X}_1, \dots, \mathbf{X}_n\}$ . Instead of adding candidates step by step, feature ranking computes an coefficient  $\mathbf{W}(\mathbf{X}_i)$  for each  $\mathbf{X}_i \in S$ , and finds a subset of  $S$  that maximizes  $\sum_{j=1}^k \mathbf{W}(\mathbf{X}_{i_j})$ , where  $i_1, \dots, i_k$  indicate the selected features. This approach avoids multivariate mutual information estimation, but ignores the interaction between different features, thus usually yields worse results than incremental selection.



Method	Dataset								Average Ranking
	Covid	Optdigits	Statlog	Gesture	Spambase	Waveform	Galaxy	Beans	
ADC [Sridhar et al., 1998]	4.36	12.81	13.63	33.70	9.85	20.84	0.75	9.10	2.9
NFIG [Setiono and Liu, 1996]	4.36	75.16	15.76	33.65	11.21	20.84	0.67	9.10	4.1
SU [Press et al., 1988]	4.34	18.33	15.46	33.65	10.13	20.84	0.63	9.10	3.1
DAS [De Mántaras, 1991]	5.76	89.16	37.30	55.55	37.71	20.84	0.8	9.10	5.8
WJE [Chi and Jabri, 1993]	5.76	22.40	20.19	48.73	24.41	20.84	0.89	9.10	5.3
RMI [Yu et al., 2019]	3.99	13.24	14.79	33.54	10.28	20.68	0.51	8.34	1.9
ARMI (Ours)	3.83	13.29	14.82	33.62	10.24	20.76	0.51	8.29	2.0

Table 4: Feature ranking results in terms of classification error (%).

Dataset	Feature Selection		Feature Ranking	
	RMI	ARMI	RMI	ARMI
Covid	2.56	0.47	0.42	0.18
Optdigits	10.68	1.25	1.45	0.61
Statlog	8.48	1.71	1.22	0.45
Gesture	86.03	8.19	12.25	2.55
Spambase	4.88	1.15	0.68	0.36
Waveform	4.43	0.77	0.64	0.30
Galaxy	8.64	1.29	1.46	0.38
Beans	30.35	3.11	4.94	0.89

Table 5: Running time (h) of RMI and ARMI on different tasks and datasets.

Again, we evaluate all methods on the same datasets shown in Table 2, with the same discretization strategy and classifier settings. We compare Rényi’s entropy based methods with previous state-of-the-art information based feature ranking criteria, including Asymmetric Dependency Coefficient[Sridhar et al., 1998](ADC), Normalized First-Order Information Gain[Setiono and Liu, 1996](NFIG), Symmetrical Uncertainty[Press et al., 1988](SU), Distance-based Attribute Selection[De Mántaras, 1991](DAS) and Weighted Joint Entropy[Chi and Jabri, 1993](WJE). For each method, 8 most informative features are selected by their corresponding ranking coefficients  $\mathbf{W}(X_i)$ . We report the comparison results in terms of classification error in Table 4, and the running time in Table 5. We can observe that ARMI still achieves 2 to 5 times speedup comparing to RMI. It is worth noting that the Galaxy dataset contains an extremely informative feature named "redshift", which leads to higher than 95% classification accuracy solely in identifying the class of a given star. Both RMI and ARMI can pick it out in the first place, but other methods even fail to choose it as the second high-weighted candidate.

### 5.2.3 Information Bottleneck for Image Classification

The Information Bottleneck (IB) objective was firstly introduced by [TISHBY, 1999] and has recently achieved great success for preventing overfitting in deep network training [Yu et al., 2021b, Ardizzone et al., 2020, Wu et al., 2020]. IB attempts to learn a representation  $\mathbf{T}$  that maximize  $\mathbf{I}(\mathbf{Y}, \mathbf{T})$  and minimize  $\mathbf{I}(\mathbf{X}, \mathbf{T})$  simultaneously, forcing the network to ignore irrelevant information of  $\mathbf{X}$  about  $\mathbf{Y}$  and thus improving robustness. IB is defined on mutual information and could be directly approximated:

$$\mathcal{L}_{IB} = \mathbf{I}(\mathbf{Y}, \mathbf{T}) - \beta \mathbf{I}(\mathbf{X}, \mathbf{T}). \quad (24)$$

When parameterizing IB with a deep neural network,  $\mathbf{X}$  denotes input variable,  $\mathbf{Y}$  denotes the desired output (e.g., class labels),  $\mathbf{T}$  refers to the latent representation of one hidden layer. Usually, this was done by optimizing the IB Lagrangian (i.e., Eq. (24)) via a classic cross-entropy loss (which amounts to  $\max \mathbf{I}(\mathbf{Y}; \mathbf{T})$  [Amjad and Geiger, 2019]) regularized by a differentiable mutual information term  $\mathbf{I}(\mathbf{X}; \mathbf{T})$ . In practice,  $I(X; T)$  can be measured by variational approximation [Alemi et al., 2016, Kolchinsky et al., 2019], mutual information neural estimator (MINE) [Belghazi et al., 2018, Elad et al., 2019] and the matrix-based Rényi’s  $\alpha$  order entropy functional [Yu et al., 2021b].

Following the experiment settings in [Alemi et al., 2016, Yu et al., 2021b], we select VGG16 [Simonyan and Zisserman, 2015] as the baseline network and CIFAR-10 as the classification dataset. We choose the last fully connected layer before softmax as the bottleneck layer. All models are trained for 400 epochs, with batch size 100, initial learning rate 0.1 reducing by a factor of 10 every 100 epochs. We follow the suggestion of [Yu et al., 2021b] and set  $\beta = 0.01$ . We evaluate the performance of IB and Approximated IB (AIB) with  $s = 20$  combined with VGG16. The final classification accuracy and time spent on calculating IB / training network are reported in Table 6.

Model	Error (%)	IB/Training Time (h)
VGG16	7.36	- / 2.27
VGG16+IB ( $\alpha = 1.01$ )	5.66	1.13 / 3.40
VGG16+IB ( $\alpha = 2$ )	5.69	
VGG16+AIB ( $\alpha = 2$ )	5.74	0.23 / 2.50

Table 6: Test error and time spent on calculating IB / training network for different methods on CIFAR-10.

For a fair comparison, we further consider the cases with  $\alpha = 1.01$  and  $\alpha = 2$ . Both cases demonstrate that AIB achieves remarkable speedup without sacrificing prediction ability, comparing to directly calculating of IB. In particular, the cost time of AIB for training VGG16 is much less than that of IB, leading to a over 5 times accelerating effect. This improvement could be further enlarged with large batch sizes, which is widely adopted in modern fine tuning techniques [Smith et al., 2018].

## 6 Conclusion

In this paper, we develop computationally efficient approximations for matrix-based Rényi’s entropy. From the viewpoint of randomized linear algebra, we design random Gaussian approximation for integer-order matrix-based Rényi’s entropy and use Taylor and Chebyshev series to approximate fractional matrix-based Rényi’s entropy. Moreover, we exploit the structure of kernel matrices to design a memory-saving block low-rank approximation for calculating the matrix-based Rényi’s entropy. Statistical guarantees are established for the proposed approximation algorithms. We also demonstrate their practical usages in real-world applications including feature selection and (multi-view) information bottleneck. In the future, we will try to acquire tighter theoretical upper bounds, and establish theoretical lower bounds for matrix-based Rényi’s entropy. We will also continue to explore more practical applications of our fast matrix-based Rényi’s entropy in both machine learning and neuroscience.

## Acknowledgments

This work was supported by National Key Research and Development Program of China(2020AAA0108800), National Natural Science Foundation of China (62106191, 12071166, 61772409, 62050194, 61721002), Innovation Research Team of Ministry of Education (IRT\_17R86), Project of China Knowledge Centre for Engineering Science and Technology and Project of Chinese academy of engineering “The Online and Offline Mixed Educational ServiceSystem for ‘The Belt and Road’ Training in MOOC China”.

## References

- Jose C Principe. *Information theoretic learning: Renyi’s entropy and kernel perspectives*. Springer Science & Business Media, 2010.
- Tongyang Li and Xiaodi Wu. Quantum Query Complexity of Entropy Estimation. *IEEE Transactions on Information Theory*, 65(5):2899–2921, 2019. ISSN 00189448. doi:10.1109/TIT.2018.2883306.
- R Devon Hjelm, Alex Fedorov, Samuel Lavoie-Marchildon, Karan Grewal, Philip Bachman, Adam Trischler, and Yoshua Bengio. Learning deep representations by mutual information estimation and maximization. *international conference on learning representations*, 2018.
- Michael Tschannen, Josip Djolonga, Paul K. Rubenstein, Sylvain Gelly, and Mario Lucic. On mutual information maximization for representation learning. *arXiv: Learning*, 2019.
- Weituo Hao Shuyang Dai Jiachang Liu Zhe Gan Cheng, Pengyu and Lawrence Carin. Club: A contrastive log-ratio upper bound of mutual information. In *International Conference on Machine Learning*, 2020.
- N TISHBY. The information bottleneck method. In *Proc. 37th Annual Allerton Conference on Communications, Control and Computing*, 1999, pages 368–377, 1999.
- Alexander A Alemi, Ian Fischer, Joshua V Dillon, and Kevin Murphy. Deep variational information bottleneck. *arXiv preprint arXiv:1612.00410*, 2016.
- Vudtiwat Ngampruetikorn and David J Schwab. Perturbation theory for the information bottleneck. *Advances in Neural Information Processing Systems*, 34, 2021.

- Jianqing Fan and Runze Li. Statistical challenges with high dimensionality. In *Proceedings of the international Congress of Mathematicians*, 2006.
- Luis Gonzalo Sanchez Giraldo, Murali Rao, and Jose C Principe. Measures of entropy from data using infinitely divisible kernels. *IEEE Transactions on Information Theory*, 61(1):535–548, 2014.
- Luis Gonzalo Sanchez Giraldo and Jose C Principe. Information theoretic learning with infinitely divisible kernels. In *International Conference on Learning Representation*, 2014.
- Austin J Brockmeier, Tingting Mu, Sophia Ananiadou, and John Y Goulermas. Quantifying the informativeness of similarity measurements. *Journal of Machine Learning Research*, 18:1–61, 2017.
- A. M. Alvarez-Meza, J. A. Lee, Michel Verleysen, and G. Castellanos-Dominguez. Kernel-based dimensionality reduction using Rényi’s  $\alpha$ -entropy measures of similarity. *Neurocomputing*, 222(April 2016):36–46, 2017. ISSN 18728286. doi:10.1016/j.neucom.2016.10.004. URL <http://dx.doi.org/10.1016/j.neucom.2016.10.004>.
- Shujian Yu, Luis Gonzalo Sanchez Giraldo, Robert Jenssen, and Jose C Principe. Multivariate extension of matrix-based rényi alpha-order entropy functional. *IEEE Transactions on Pattern Analysis and Machine Intelligence*, 42(11):2960–2966, 2019.
- Kristoffer Wickstrøm, Sigurd Løkse, Michael Kampffmeyer, Shujian Yu, Jose Principe, and Robert Jenssen. Information Plane Analysis of Deep Neural Networks via Matrix-Based Rényi’s Entropy and Tensor Kernels. (2017), 2019. URL <http://arxiv.org/abs/1909.11396>.
- Shujian Yu, Francesco Alesiani, Xi Yu, Robert Jenssen, and Jose Principe. Measuring dependence with matrix-based entropy functional. In *Association for the Advancement of Artificial Intelligence*, 2021a.
- Michael Elad. *Sparse and redundant representations: from theory to applications in signal and image processing*. Springer, 2010.
- Mu Li, Wei Bi, James T Kwok, and Bao-Liang Lu. Large-scale nyström kernel matrix approximation using randomized svd. *IEEE Transactions on Neural Networks and Learning Systems*, 26(1):152–164, 2014.
- Michael W Mahoney and Petros Drineas. Cur matrix decompositions for improved data analysis. *Proceedings of the National Academy of Sciences*, 106(3):697–702, 2009.
- Michael W Mahoney. Randomized algorithms for matrices and data. *Foundations and Trends in Machine Learning*, 3(2), 2011.
- David S Watkins. The qr algorithm revisited. *SIAM review*, 50(1):133–145, 2008.
- David S Watkins. *Fundamentals of matrix computations*, volume 64. John Wiley & Sons, 2004.
- Haim Avron and Sivan Toledo. Randomized algorithms for estimating the trace of an implicit symmetric positive semi-definite matrix. *Journal of the ACM (JACM)*, 58(2):1–34, 2011.
- George J Klir and Mark J Wierman. *Uncertainty-based information: elements of generalized information theory*, volume 15. Physica, 2013.
- Rajendra Bhatia. Infinitely divisible matrices. *The American Mathematical Monthly*, 113(3):221–235, 2006.
- Christos Boutsidis, Petros Drineas, Prabhanjan Kambadur, Eugenia-Maria Kontopoulou, and Anastasios Zouzias. A randomized algorithm for approximating the log determinant of a symmetric positive definite matrix. *Linear Algebra and its Applications*, 533:95–117, 2017.
- Charles W Clenshaw. A note on the summation of chebyshev series. *Mathematics of Computation*, 9(51):118–120, 1955.
- Si Si, Cho-Jui Hsieh, and Inderjit S. Dhillon. Memory efficient kernel approximation. *Journal of Machine Learning Research*, 18(20):1–32, 2017.
- N. Halko, P. G. Martinsson, and J. A. Tropp. Finding structure with randomness: Probabilistic algorithms for constructing approximate matrix decompositions. *SIAM Review*, 53(2):217–288, 2011. ISSN 00361445. doi:10.1137/090771806.
- Sourav Das. Inequalities for q-gamma function ratios. *Analysis and Mathematical Physics*, 9(1):313–321, 2019. ISSN 1664235X. doi:10.1007/s13324-017-0198-0.
- Wen Li and Weiwei Sun. The perturbation bounds for eigenvalues of normal matrices. *Numerical Linear Algebra with Applications*, 12(2-3):89–94, 2005. ISSN 10705325. doi:10.1002/nla.400.
- G. Bradski. The OpenCV Library. *Dr. Dobb’s Journal of Software Tools*, 2000.
- Gaël Guennebaud, Benoît Jacob, et al. Eigen v3. <http://eigen.tuxfamily.org>, 2010.

- Adam Paszke, Sam Gross, Francisco Massa, Adam Lerer, James Bradbury, Gregory Chanan, Trevor Killeen, Zeming Lin, Natalia Gimelshein, Luca Antiga, Alban Desmaison, Andreas Köpf, Edward Yang, Zach DeVito, Martin Raison, Alykhan Tejani, Sasank Chilamkurthy, Benoit Steiner, Lu Fang, Junjie Bai, and Soumith Chintala. PyTorch: An imperative style, high-performance deep learning library. *Advances in Neural Information Processing Systems*, 32 (NeurIPS), 2019. ISSN 10495258.
- Dheeru Dua and Casey Graff. UCI machine learning repository, 2017. URL <http://archive.ics.uci.edu/ml>.
- Murat Koklu and Ilker Ali Ozkan. Multiclass classification of dry beans using computer vision and machine learning techniques. *Computers and Electronics in Agriculture*, 174(May):105507, 2020. ISSN 01681699. doi:10.1016/j.compag.2020.105507. URL <https://doi.org/10.1016/j.compag.2020.105507>.
- Bela Abolfathi, D. S. Aguado, and et al. The Fourteenth Data Release of the Sloan Digital Sky Survey: First Spectroscopic Data from the Extended Baryon Oscillation Spectroscopic Survey and from the Second Phase of the Apache Point Observatory Galactic Evolution Experiment. *The Astrophysical Journal Supplement Series*, 235(2):42, 2018. ISSN 0067-0049. doi:10.3847/1538-4365/aa9e8a.
- Nguyen Xuan Vinh, Shuo Zhou, Jeffrey Chan, and James Bailey. Can high-order dependencies improve mutual information based feature selection? *Pattern Recognition*, 53:46–58, 2016. ISSN 00313203. doi:10.1016/j.patcog.2015.11.007.
- R. Battiti. Using mutual information for selecting features in supervised neural net learning. *IEEE Transactions on Neural Networks*, 5(4):537–550, 1994.
- Gavin Brown. A new perspective for information theoretic feature selection. *Journal of Machine Learning Research*, 5(1):49–56, 2009. ISSN 15324435.
- David D. Lewis. Feature selection and feature extraction for text categorization. *Proceedings of the workshop on Speech and Natural Language*, page 212, 1992. doi:10.3115/1075527.1075574.
- Hanchuan Peng, Fuhui Long, and Chris Ding. Feature selection based on mutual information criteria of max-dependency, max-relevance, and min-redundancy. *IEEE Transactions on pattern analysis and machine intelligence*, 27(8):1226–1238, 2005.
- H Yang. Data visualization and feature selection: New algorithms for nongaussian data. *Advances in Neural Information Processing Systems*, (Mi):687—693, 1999.
- Francois Fleuret. Fast binary feature selection with conditional mutual information. *Journal of Machine learning research*, 5(9), 2004.
- Nguyen Xuan Vinh, Jeffrey Chan, and James Bailey. Reconsidering mutual information based feature selection: A statistical significance view. *Proceedings of the National Conference on Artificial Intelligence*, 3(1):2092–2098, 2014.
- Chih-Chung Chang and Chih-Jen Lin. Libsvm: A library for support vector machines. *ACM transactions on intelligent systems and technology (TIST)*, 2(3):1–27, 2011.
- Dasaratha V. Sridhar, Eric B. Bartlett, and Richard C. Seagrave. Information theoretic subset selection for neural network models. *Computers and Chemical Engineering*, 22(4-5):613–626, 1998. ISSN 00981354. doi:10.1016/s0098-1354(97)00227-5.
- Rudy Setiono and Huan Liu. Improving backpropagation learning with feature selection. *Applied Intelligence*, 6(2): 129–139, 1996. ISSN 0924669X. doi:10.1007/BF00117813.
- William H Press, Saul A Teukolsky, William T Vetterling, and Brian P Flannery. Numerical recipes in c, 1988.
- R. López De Mántaras. A Distance-Based Attribute Selection Measure for Decision Tree Induction. *Machine Learning*, 6(1):81–92, 1991. ISSN 15730565. doi:10.1023/A:1022694001379.
- Jabri Chi and M Jabri. Entropy based feature evaluation and selection technique. In *Proc. of 4th Australian Conf. on Neural Networks (ACNN’93)*, pages 181–196, 1993.
- Xi Yu, Shujian Yu, and Jose C. Principe. Deep Deterministic Information Bottleneck with Matrix-Based Entropy Functional. *IEEE International Conference on Acoustics, Speech and Signal Processing (ICASSP)*, pages 3160–3164, 2021b. doi:10.1109/icassp39728.2021.9414151.
- Lynton Ardizzone, Radek Mackowiak, Carsten Rother, and Ullrich Köthe. Training normalizing flows with the information bottleneck for competitive generative classification. *Advances in Neural Information Processing Systems*, 2020-December(1):1–13, 2020. ISSN 10495258.
- Tailin Wu, Hongyu Ren, Pan Li, and Jure Leskovec. Graph information bottleneck. *Advances in Neural Information Processing Systems*, 2020-December(NeurIPS), 2020. ISSN 10495258.

- Rana Ali Amjad and Bernhard C Geiger. Learning representations for neural network-based classification using the information bottleneck principle. *IEEE transactions on pattern analysis and machine intelligence*, 42(9):2225–2239, 2019.
- Artemy Kolchinsky, Brendan D Tracey, and David H Wolpert. Nonlinear information bottleneck. *Entropy*, 21(12):1181, 2019.
- Mohamed Ishmael Belghazi, Aristide Baratin, Sai Rajeshwar, Sherjil Ozair, Yoshua Bengio, Aaron Courville, and Devon Hjelm. Mutual information neural estimation. In *International Conference on Machine Learning*, pages 531–540. PMLR, 2018.
- Adar Elad, Doron Haviv, Yochai Blau, and Tomer Michaeli. Direct validation of the information bottleneck principle for deep nets. In *Proceedings of the IEEE/CVF International Conference on Computer Vision Workshops*, pages 0–0, 2019.
- Karen Simonyan and Andrew Zisserman. Very deep convolutional networks for large-scale image recognition. *3rd International Conference on Learning Representations, ICLR 2015 - Conference Track Proceedings*, pages 1–14, 2015.
- Samuel L. Smith, Pieter-Jan Kindermans, and Quoc V. Le. Don’t decay the learning rate, increase the batch size. In *International Conference on Learning Representations*, 2018. URL <https://openreview.net/forum?id=B1Yy1BxCZ>.

## A Power Iteration Algorithm

The power iteration algorithm is a well-known method to compute the largest eigenvalue of large-scale matrices. Lemma 3 establishes the theoretical bound of Algorithm 5.

---

**Algorithm 5** Power Iteration [Boutsidis et al., 2017]

---

- 1: **Input:** Positive semi-definite matrix  $G \in \mathbb{R}^{n \times n}$ , integers  $q, t > 0$ .
  - 2: **for**  $j = 1, \dots, q$  **do**
  - 3:   Randomly select a vector  $\mathbf{x}_0^j \in \{-1, +1\}^n$ .
  - 4:   **for**  $i = 1, \dots, t$  **do**
  - 5:      $\mathbf{x}_i^j = G \cdot \mathbf{x}_{i-1}^j$ .
  - 6:   **end for**
  - 7:   Compute  $\tilde{\lambda}_j = \frac{\mathbf{x}_t^{j\top} G \mathbf{x}_t^j}{\mathbf{x}_t^{j\top} \mathbf{x}_t^j}$ .
  - 8: **end for**
  - 9: **Output:**  $\tilde{\lambda}_{max} = \max_{j=1, \dots, q} \tilde{\lambda}_j$ .
- 

**Lemma 3** [Boutsidis et al., 2017] Let  $\tilde{\lambda}_{max}$  be the output of Algorithm 5 with  $q = \lceil 4.82 \log(1/\delta) \rceil$  and  $t = \lceil \log \sqrt{4n} \rceil$ , then with probability at least  $1 - \delta$ :

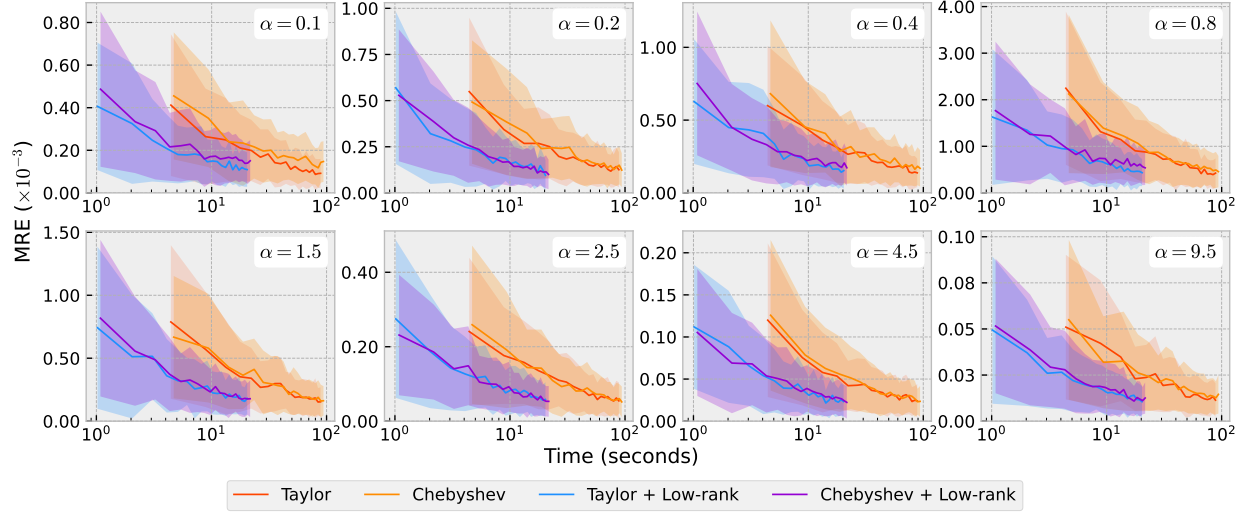
$$\frac{1}{6} \lambda_{min} \leq \tilde{\lambda}_{max} \leq \lambda_{min}.$$

The time complexity of computing the largest eigenvalue is thus  $O(\text{nnz}(G) \log n \log(1/\delta))$ . It is usually marginal comparing to the complexity of trace estimation, so we ignore it in our main analysis for simplicity.

## B Supplementary Experiment Results

### B.1 Taylor & Chebyshev Series Approximation

Additionally, we report the results for time vs. MRE curves of all approximation methods with  $\sigma = 0.5$  in Gaussian kernel. we keep the previous experiment settings and set  $m = 40$ ,  $c = 15$ . The results are shown in Figure 6 and Table 7.


 Figure 6: Time vs. MRE curves for fractional  $\alpha$ -order Rényi's entropy estimation with  $\sigma = 0.5$ .

Method	$\alpha$		0.1	0.4	1.5	4.5
	Time (s)		0.2	0.8	2.5	9.5
Eigenvalue	219.8		-			
Taylor	88.5		$0.087 \pm 0.074$	$0.138 \pm 0.098$	$0.152 \pm 0.112$	$0.023 \pm 0.017$
Chebyshev	93.7		$0.117 \pm 0.090$	$0.404 \pm 0.321$	$0.054 \pm 0.041$	$0.011 \pm 0.009$
Taylor + Low-rank	20.4		$0.118 \pm 0.094$	$0.169 \pm 0.125$	$0.162 \pm 0.116$	$0.023 \pm 0.015$
Chebyshev + Low-rank	21.6		$0.123 \pm 0.092$	$0.456 \pm 0.338$	$0.052 \pm 0.041$	$0.013 \pm 0.009$
			$0.107 \pm 0.078$	$0.142 \pm 0.102$	$0.157 \pm 0.114$	$0.023 \pm 0.017$
			$0.095 \pm 0.082$	$0.434 \pm 0.289$	$0.056 \pm 0.041$	$0.011 \pm 0.008$
			$0.138 \pm 0.088$	$0.173 \pm 0.123$	$0.176 \pm 0.126$	$0.022 \pm 0.019$
			$0.100 \pm 0.080$	$0.538 \pm 0.369$	$0.053 \pm 0.041$	$0.011 \pm 0.007$

 Table 7: Time and  $\text{MRE} \times 10^{-3}$  ( $\text{SD} \times 10^{-3}$ ) for fractional  $\alpha$ -order Rényi's entropy estimation with  $\sigma = 0.5$ .

## B.2 Feature Selection

We additionally report number of features vs. classification accuracy curves for all feature selection methods on 8 different datasets shown in Figure 7. Those for feature ranking methods are shown in 8. It can be seen that classification error is stable and directly comparable after selecting 8 features.

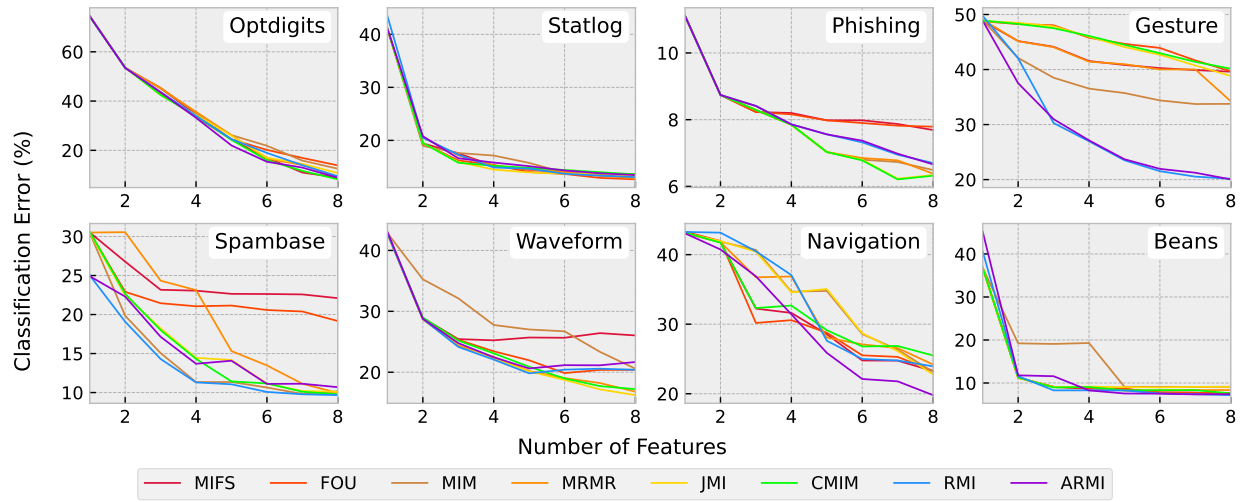


Figure 7: Number of Features vs. Classification Error curves for feature selection methods.

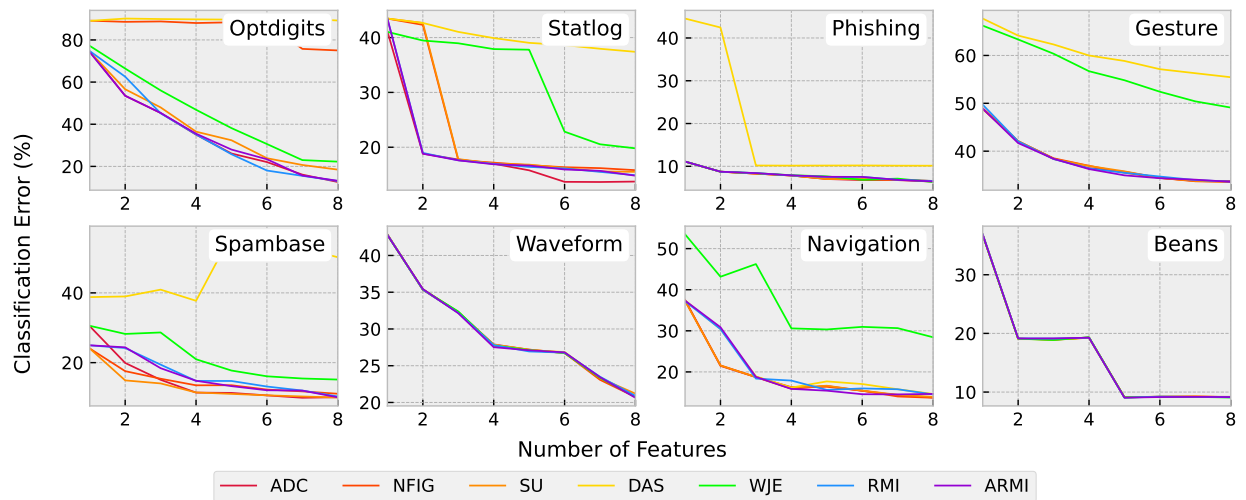


Figure 8: Number of Features vs. Classification Error curves for feature ranking methods.